Day 3 - Artifacts, Noise, Optimization

CBIC MRI Bootcamp 2025

Mike Tyszka
Caltech Brain Imaging Center

Caltech

Review

- MRI tissue contrast primarily from **proton density, T1, T2 and T2* relaxation**
- Gradient Echo images are **sensitive** to B0 inhomogeneities
- Spin Echo images are **insensitive** to B0 inhomogeneities
- **Band-limited RF pulses** allow volume/slice selection
- Four workhorse fMRI pulse sequences:
  - MP-RAGE (T1w Structural)
  - SPACE (T2w Structural)
  - SE-EPI (T2w Field-mapping)
  - GRE-EPI (T2*w Functional)

Sources of Noise in MRI

- **Participant's Body**
  - Important at lower fields/larger subjects
- **RF Receive Coil**
  - Important at higher fields/smaller samples
- **RF Preamplifier and Receiver Electronics**
- **External Sources**
  - Electromagnetic Interference or **EMI**

Internal Noise Sources

- **Participant's Body**
  - RF black body radiation (37º core temp)
  - Physiological noise (heart beat, breathing, etc)
- **Scanner Hardware**
  - Dominated by thermal Johnson-Nyquist noise
  - Temperature dependent with Gaussian white distribution
  - RF coil conductors, preamps, ADCs etc

Gaussian White Noise

Pixel noise values drawn from Gaussian/Normal distribution $X_i \sim N(\mu, \sigma)$

Noise is additive in k-space

Independent for real and imaginary channels

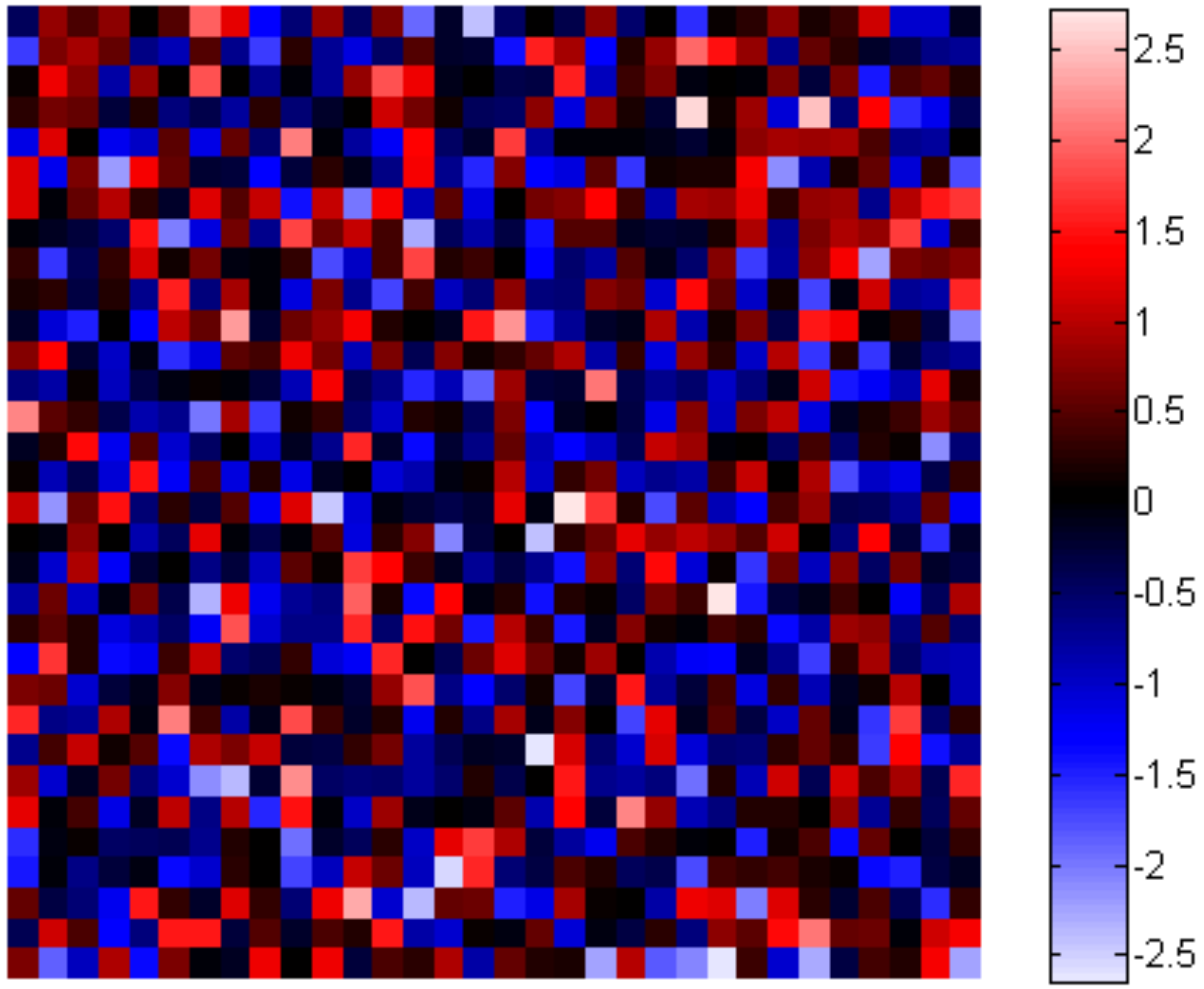

$N(0,1)$

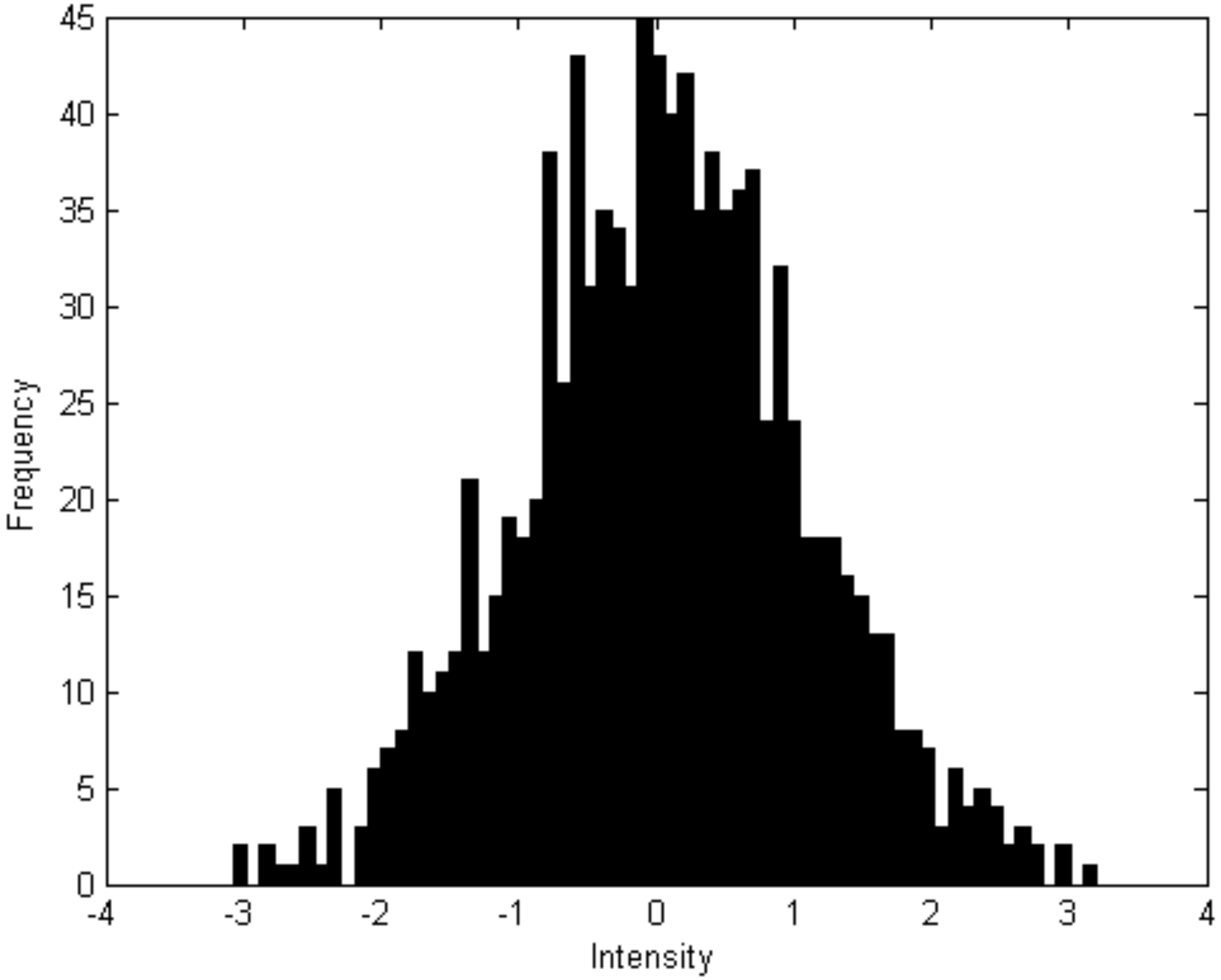

Rayleigh and Rician Noise

The absolute value of Gaussian white noise has a Rayleigh distribution with mean > 0

The absolute value of signal with added Gaussian white noise has a Rician distribution

As SNR increases the Rician distributed signal approaches a Gaussian distribution

Absolute Gaussian Noise

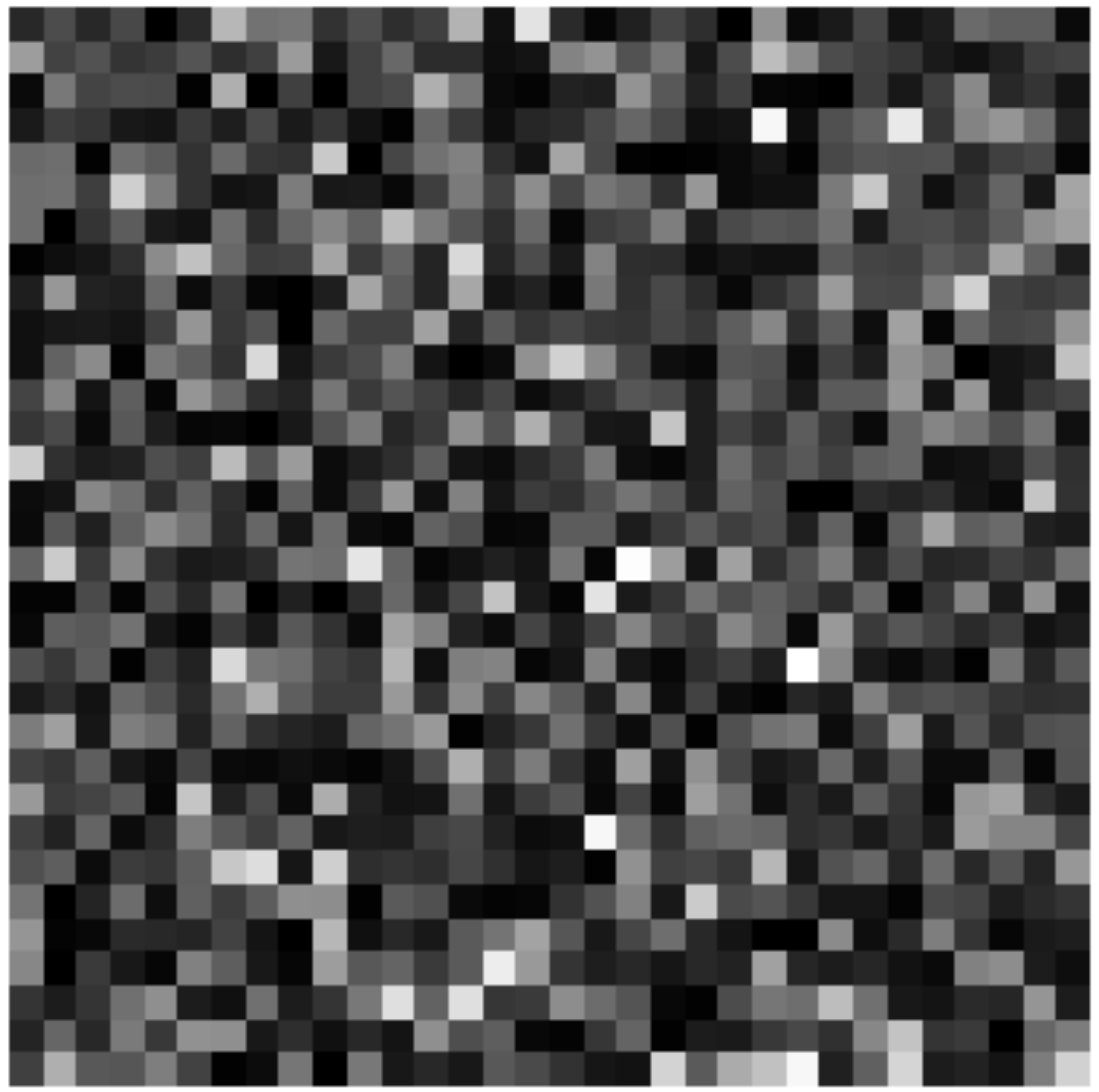

Rayleigh noise distribution

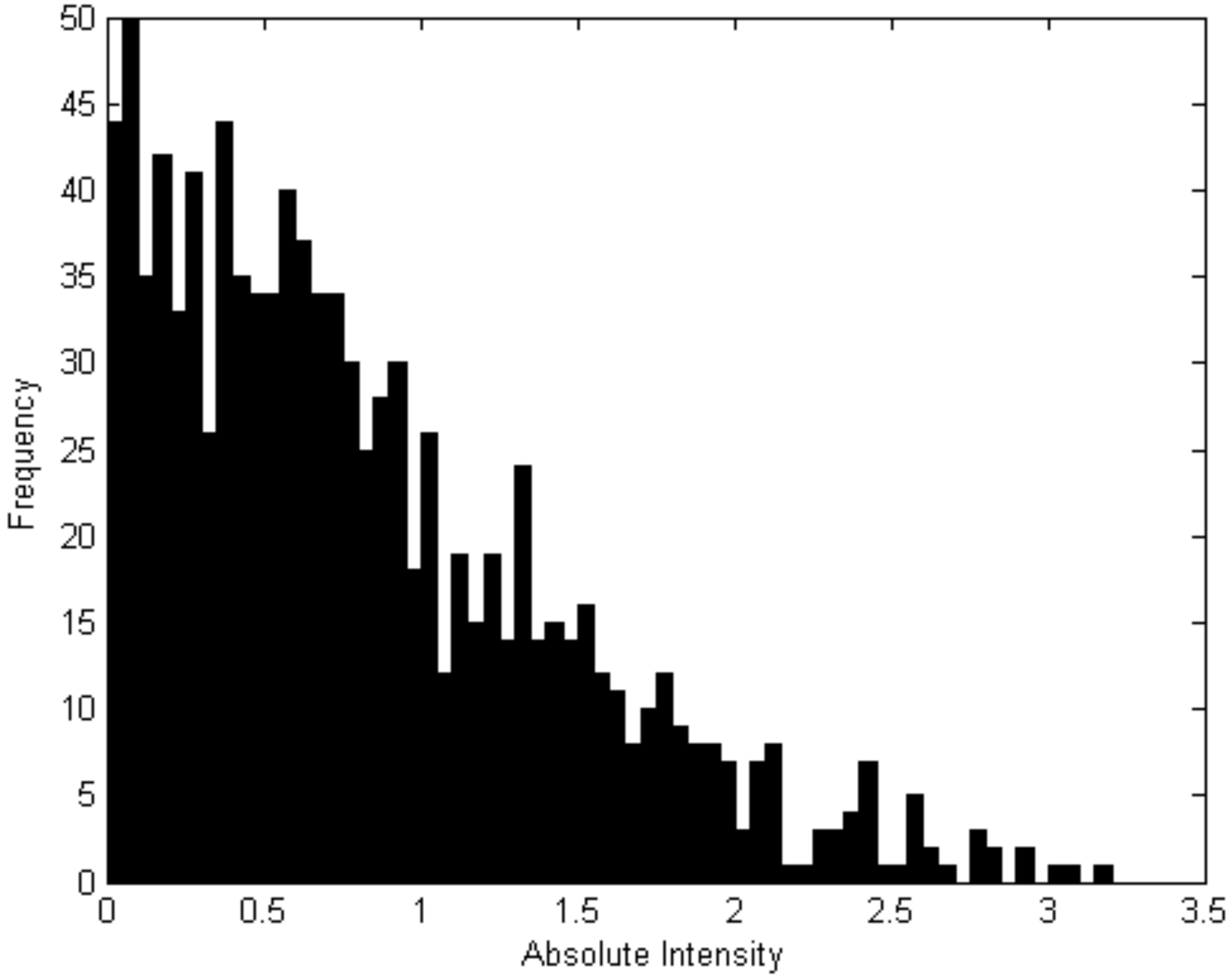

Contrast-to-noise Ratio

CNR tends to be more important than raw SNR in structural images

Temporal CNR important metric for BOLD fMRI

SNR = 20
CNR = 2

SNR = 10
CNR = 2

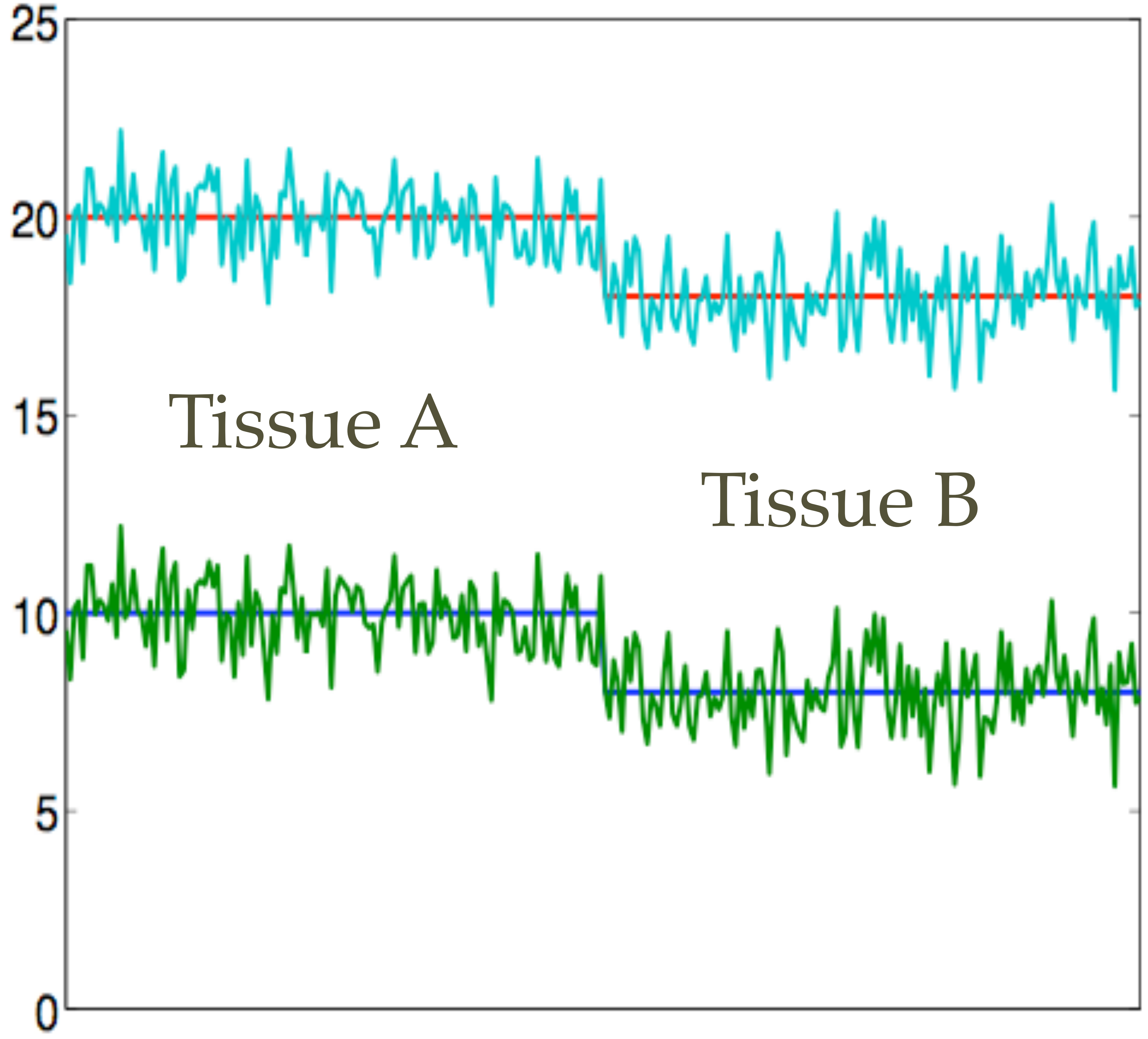

Estimating image noise

- **Spatial noise**
  - Use air space without artifacts (S_{air})
  - Gaussian White Noise SD = 1.48 * MAD(S_{air})
- **Temporal noise**
  - Need to remove low frequency components (HPF)
  - Strictly temporal signal-to-fluctuation noise (tSFNR)

Spatial Noise Estimation

Typical window

Noise window

Noise ROI well away from signal and artifacts

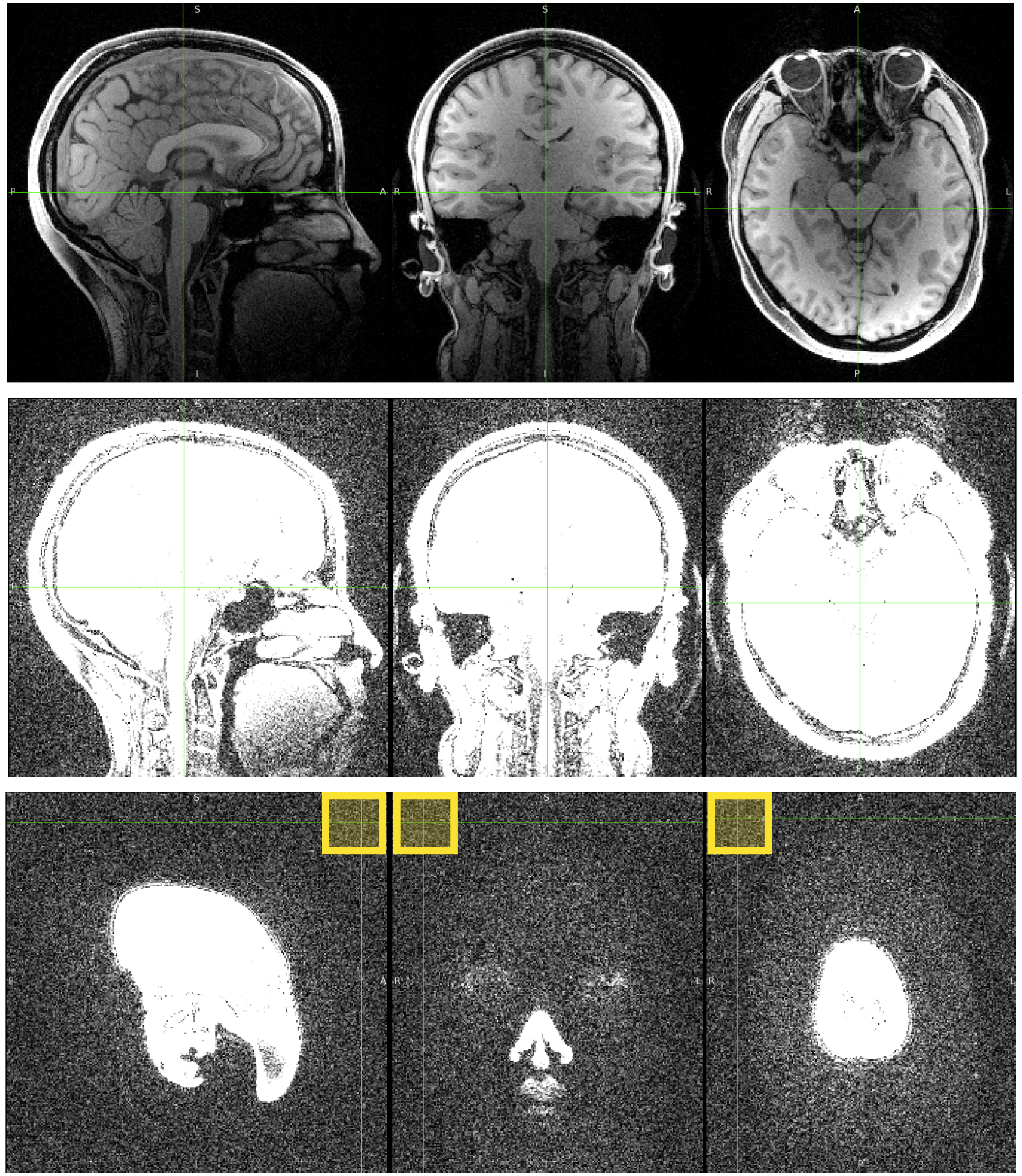

For Gaussian white noise

$$\hat{\sigma}_n = 1.48 \ \mathrm{median}(|S_i|)$$

Temporal SNR

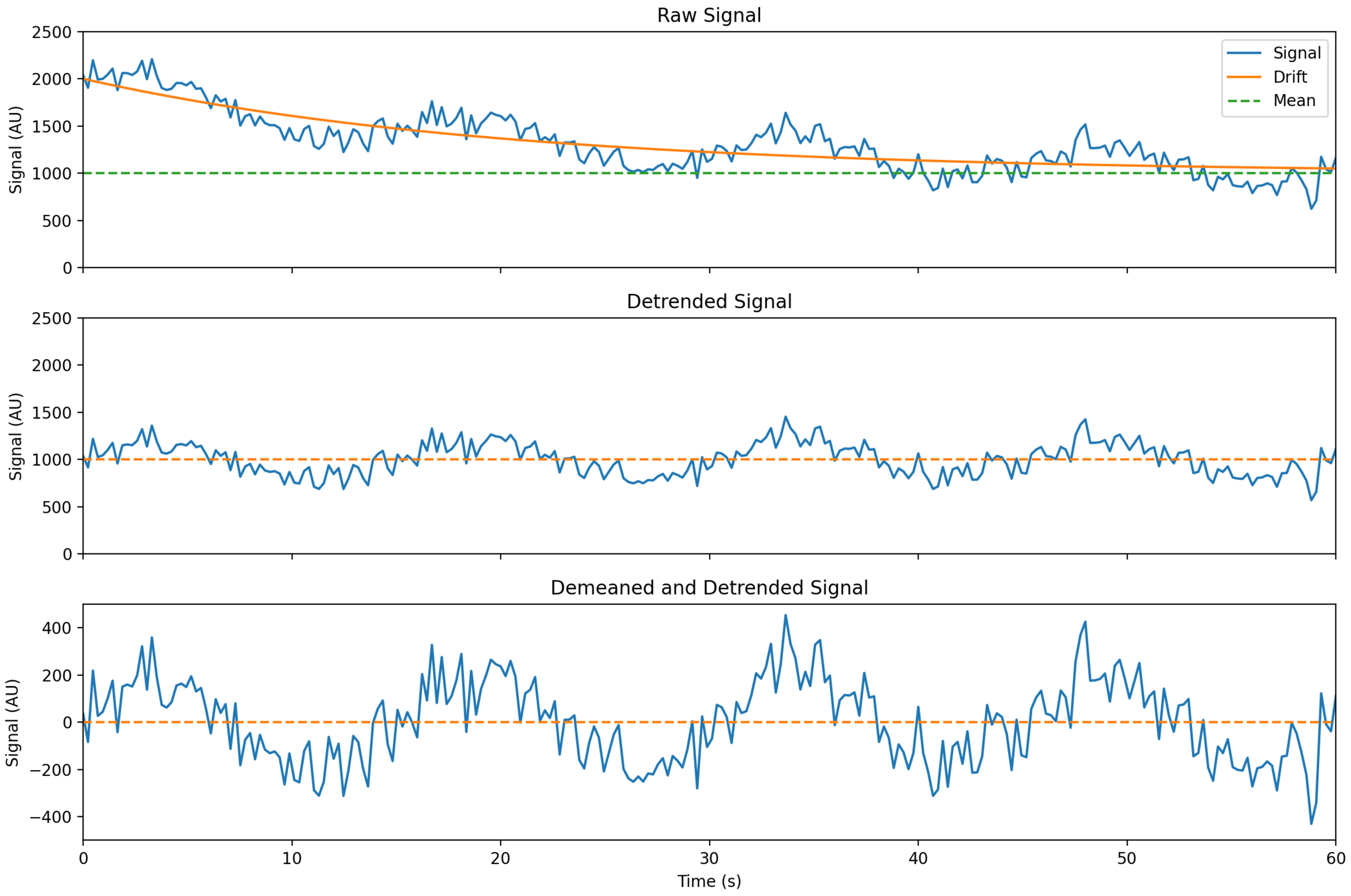

tSFNR Efficiency

Compare apples with apples

Adjust SNR for voxel volume and TR

Useful for comparing sequences with different imaging parameters for the same purpose

$$\eta' = \frac{\text{tSNR}}{V\sqrt{\tau}}$$

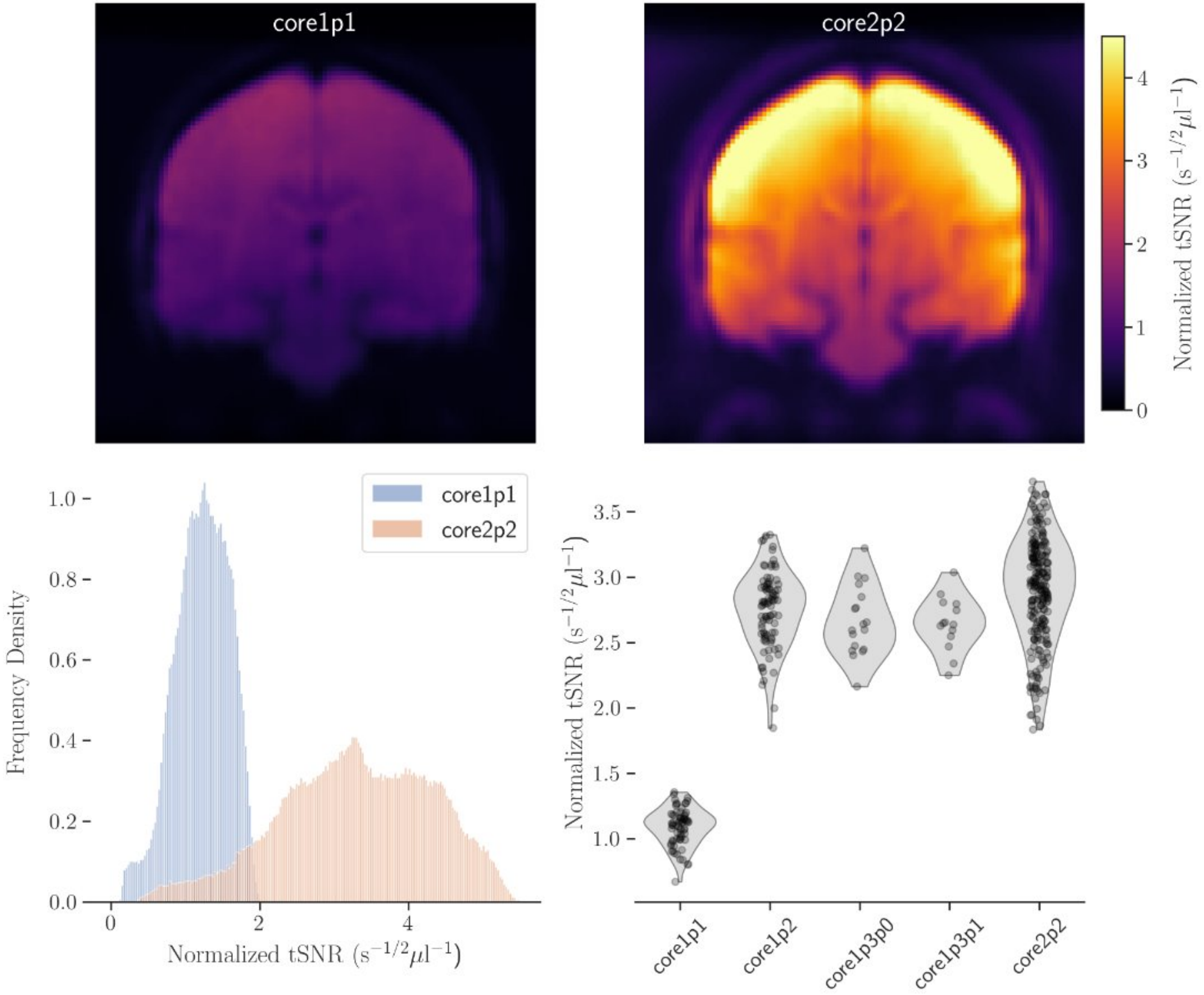

Incoherent Interference

Typically external EMI sources like unsuppressed electric motors, welding, etc

Unlikely to be narrow band or phase coherent with k-space acquisition

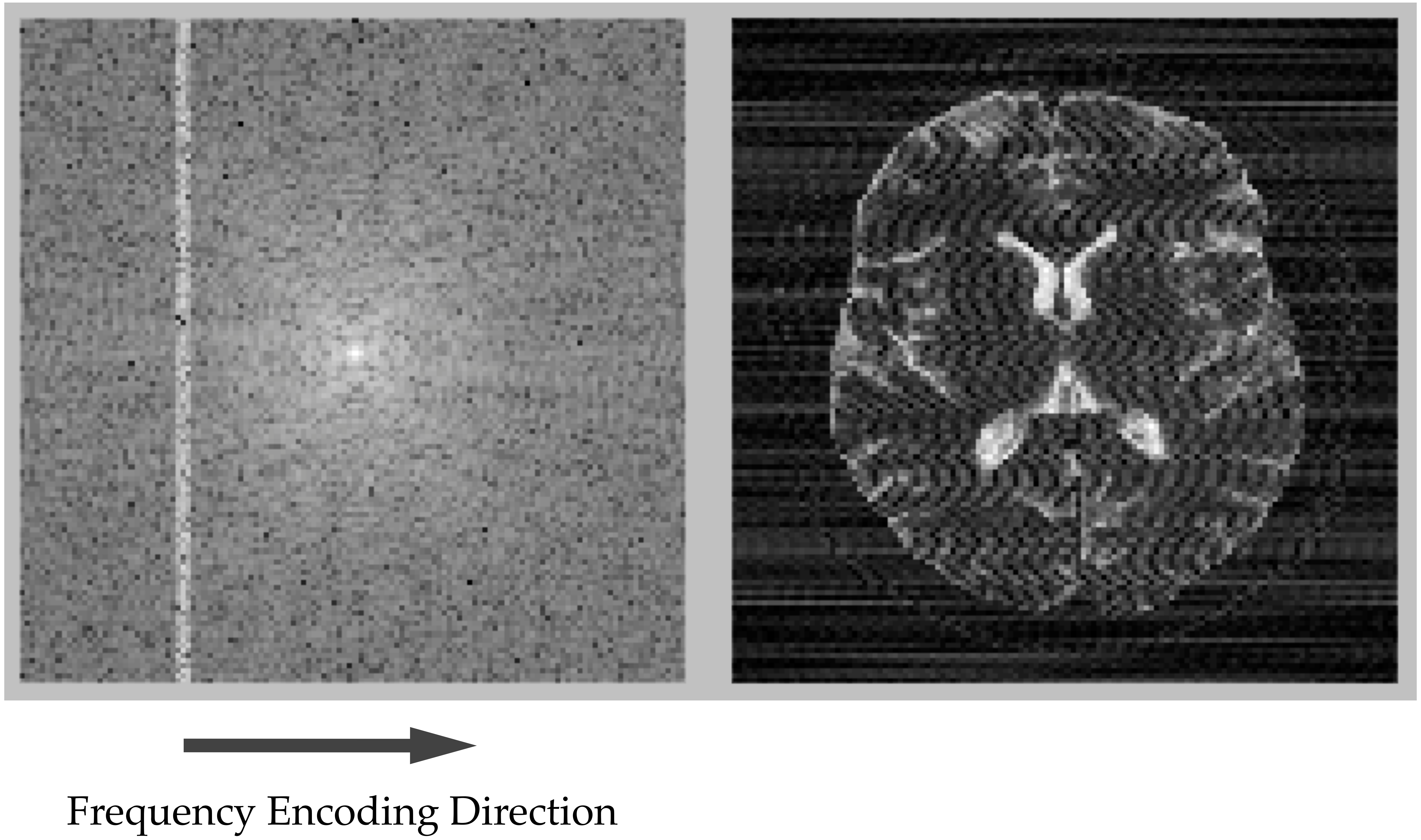

Coherent Interference

Very short interference event

Spark discharge

Narrow frequency band

No phase coherence with acquisition

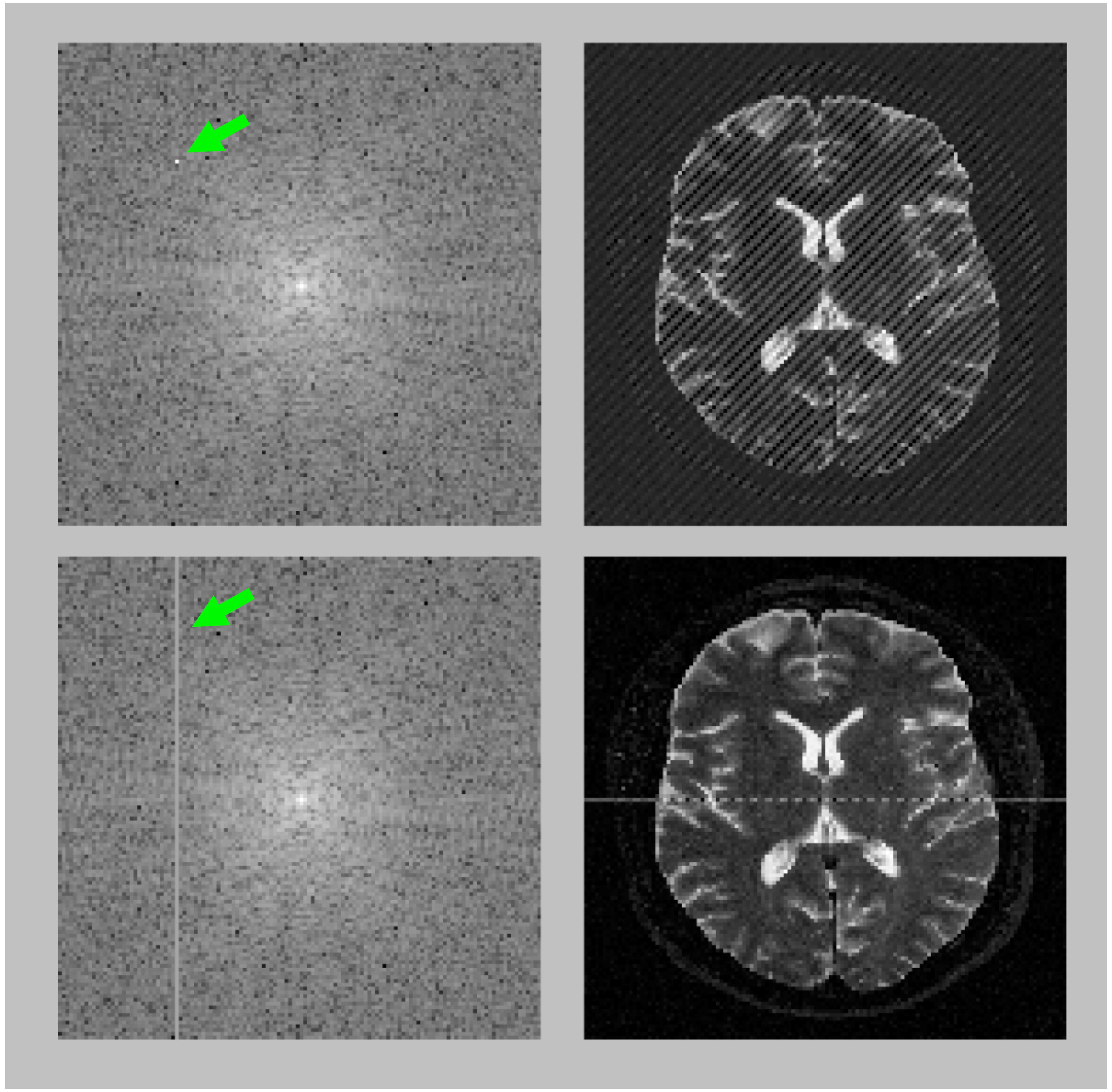

Corduroy Artifact

Zipper Artifact

Image Artifacts

- MR image artifacts break reconstruction assumptions
- Typical **assumptions** for MR image reconstruction
  - Tissue is stationary
  - Magnetic fields (B0 and B1) are perfectly homogeneous
  - Actual k-space trajectory matches expected trajectory
  - Signal doesn't decay during data acquisition

Stationary Tissue Assumption : Motion Artifacts

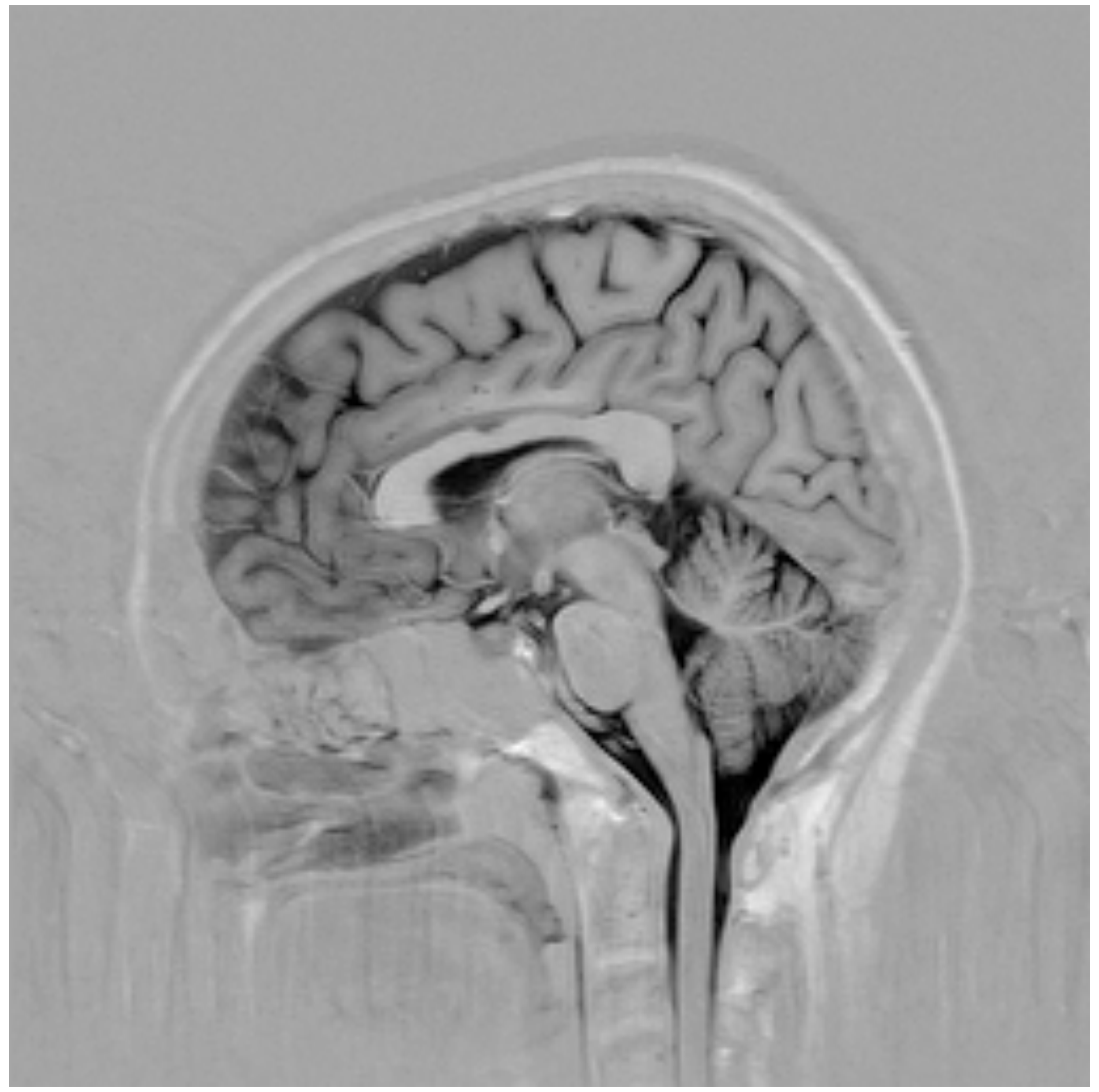
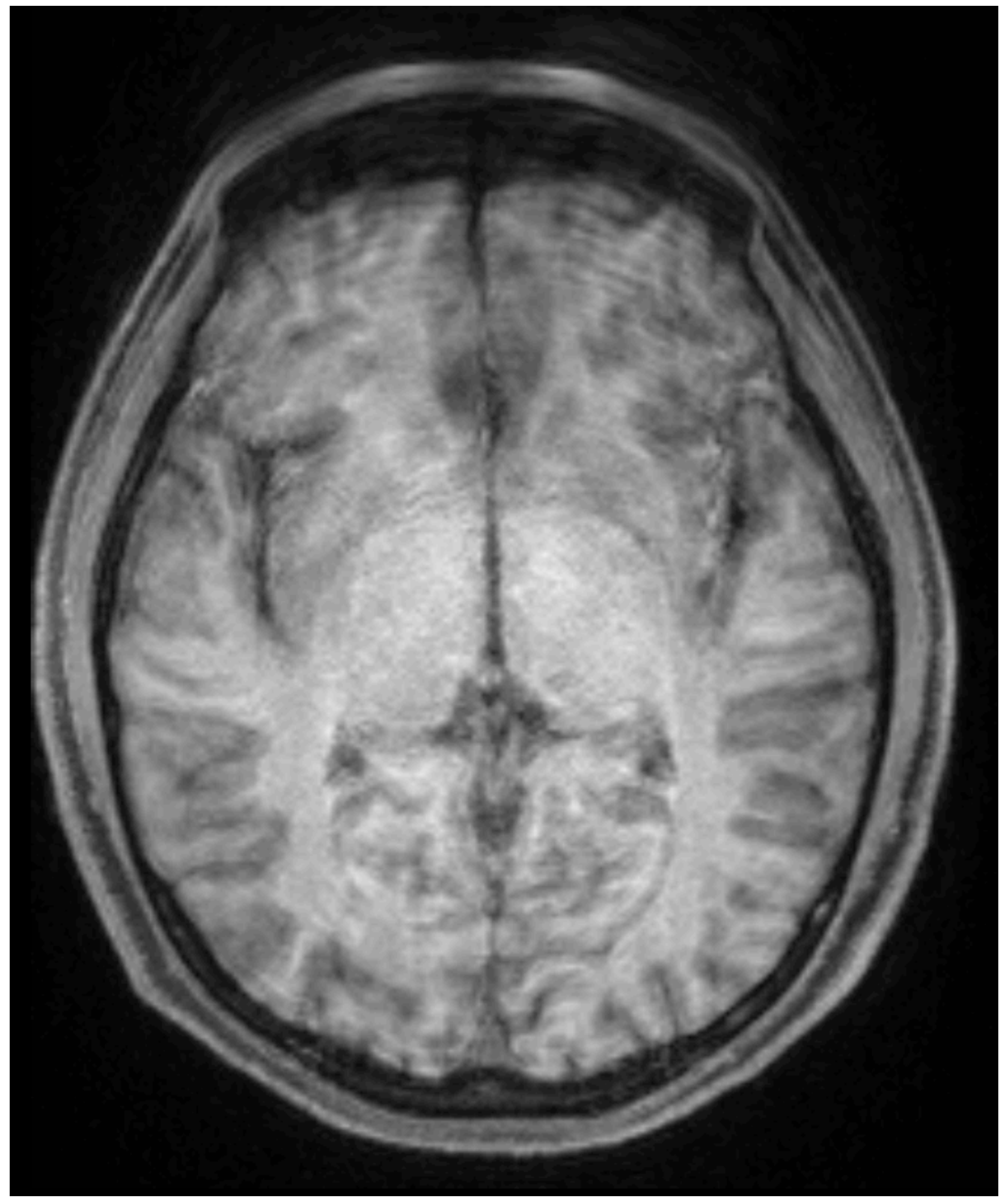
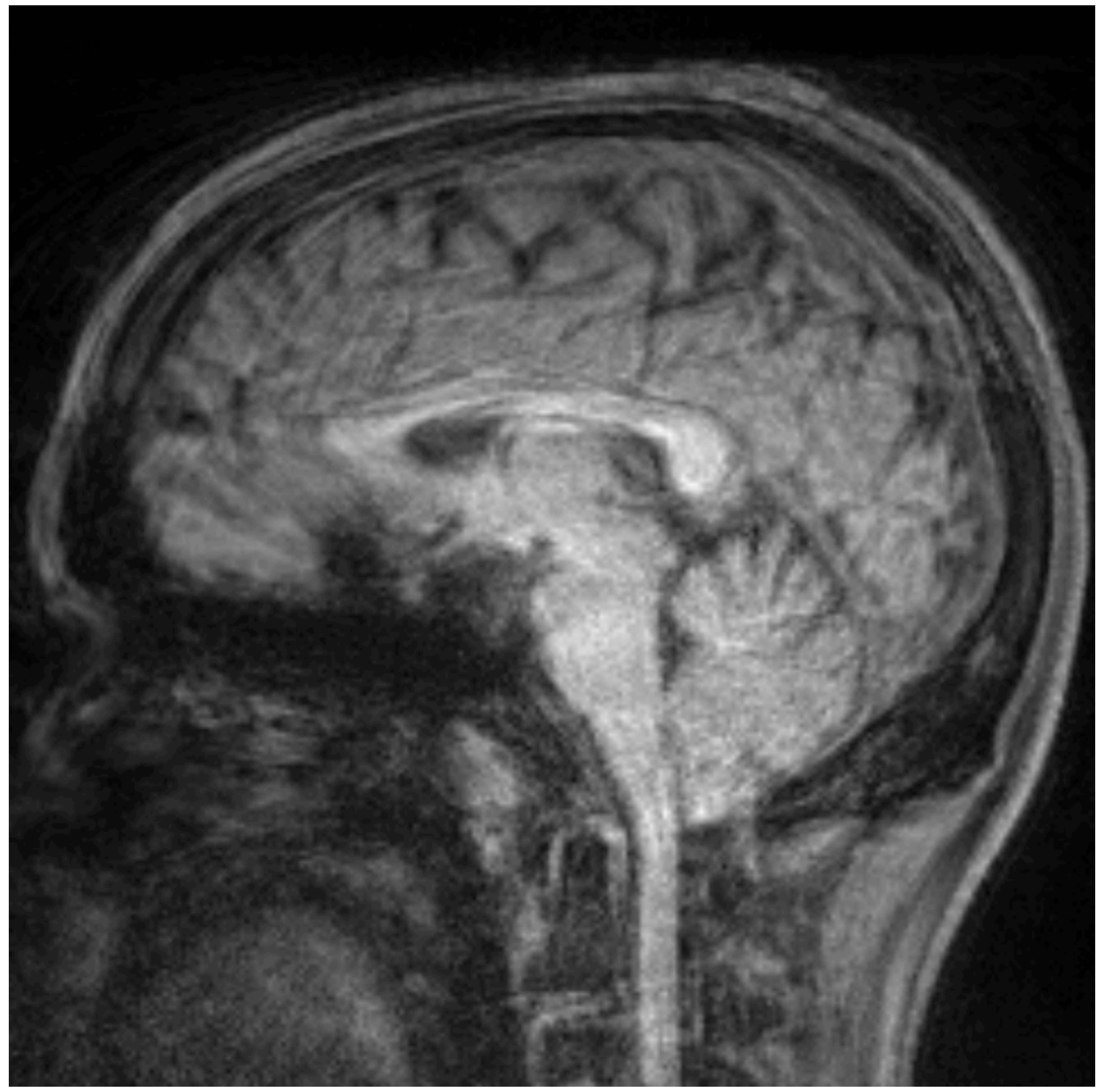
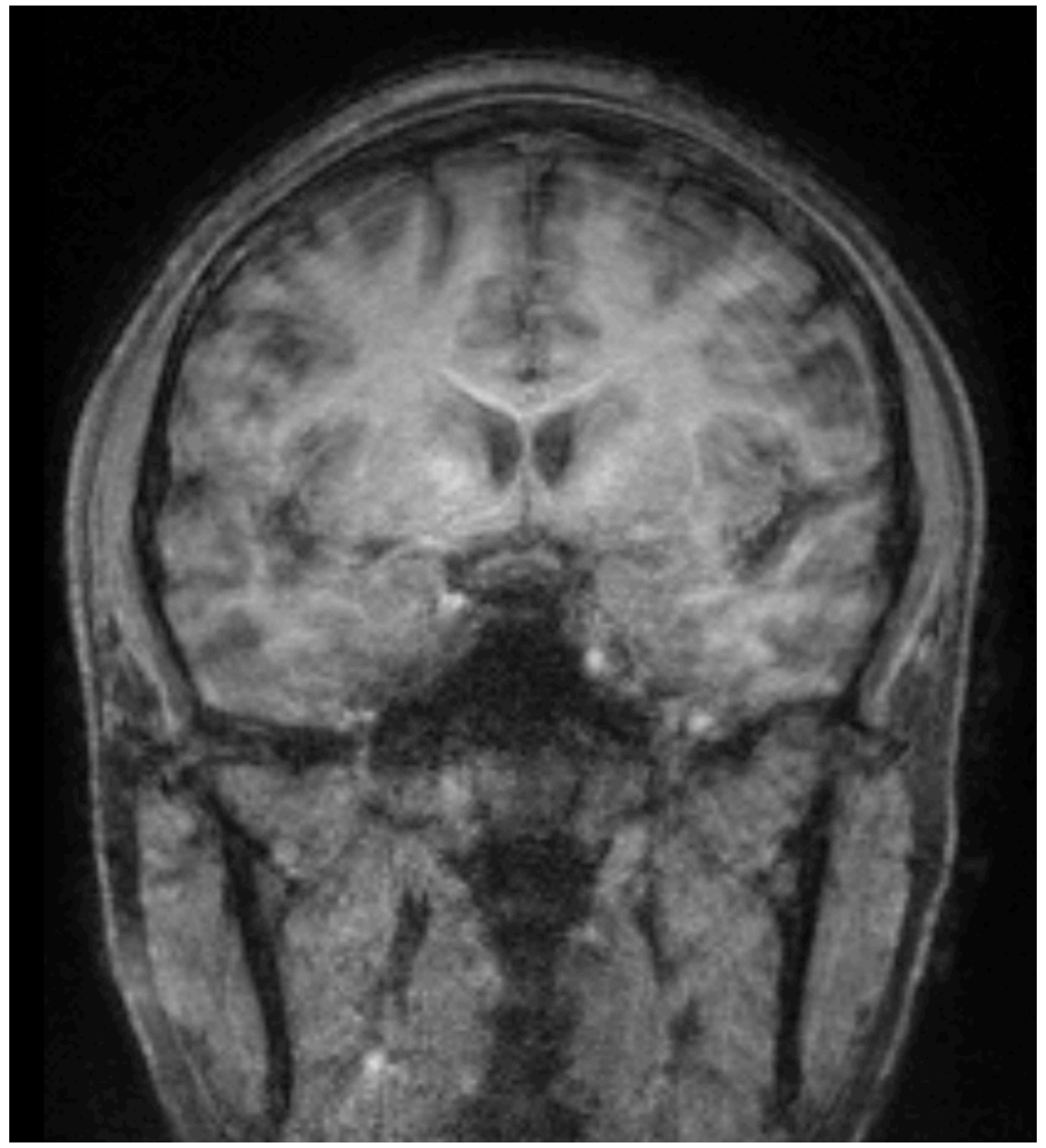

Arise from departure of actual transverse magnetization phase of moving material from expected phase of stationary material. Ghost artifacts seen in phase encoding direction.

B0 Homogeneity and Ferromagnetic Materials

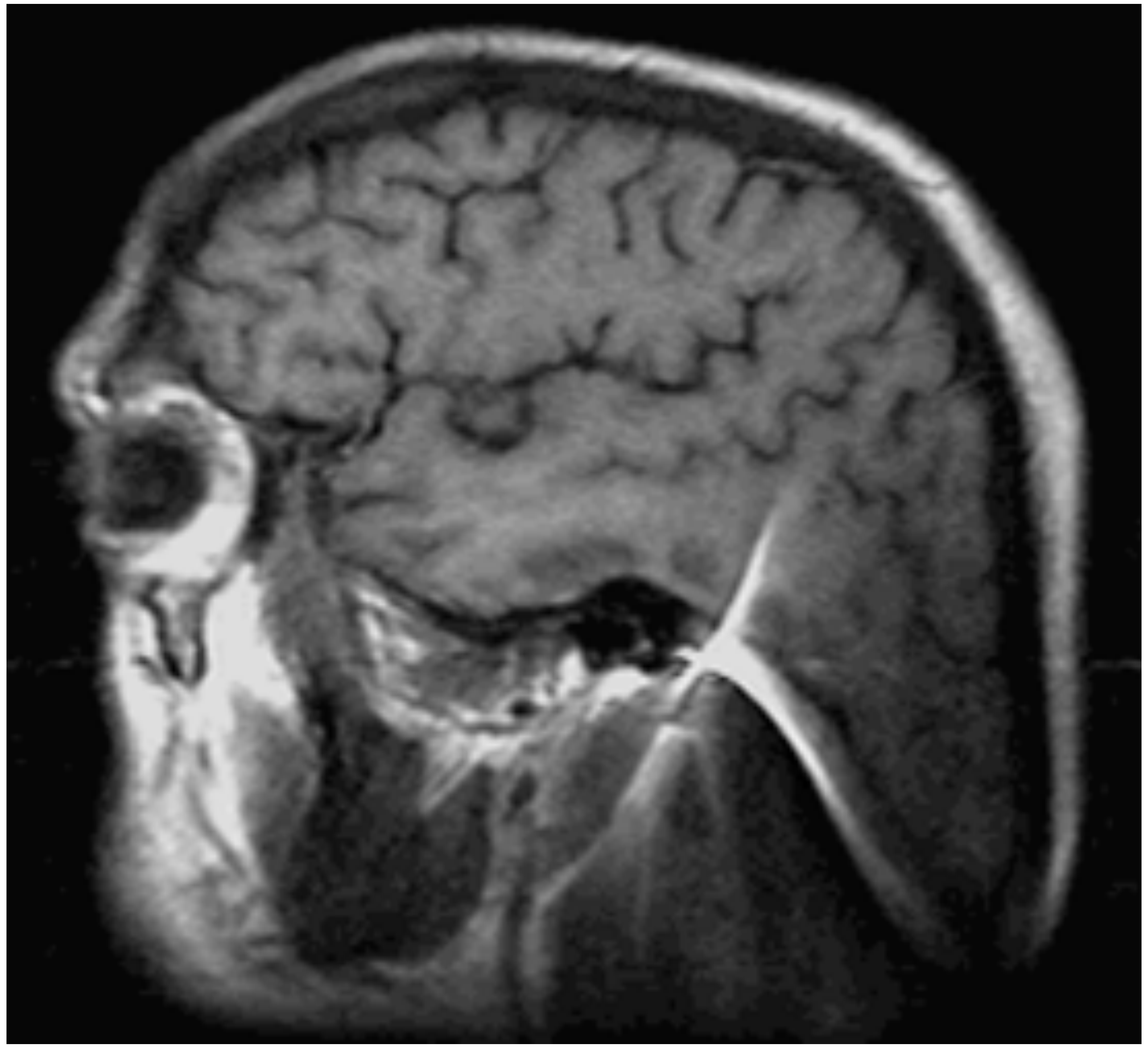

Natural B0 Inhomogeneity

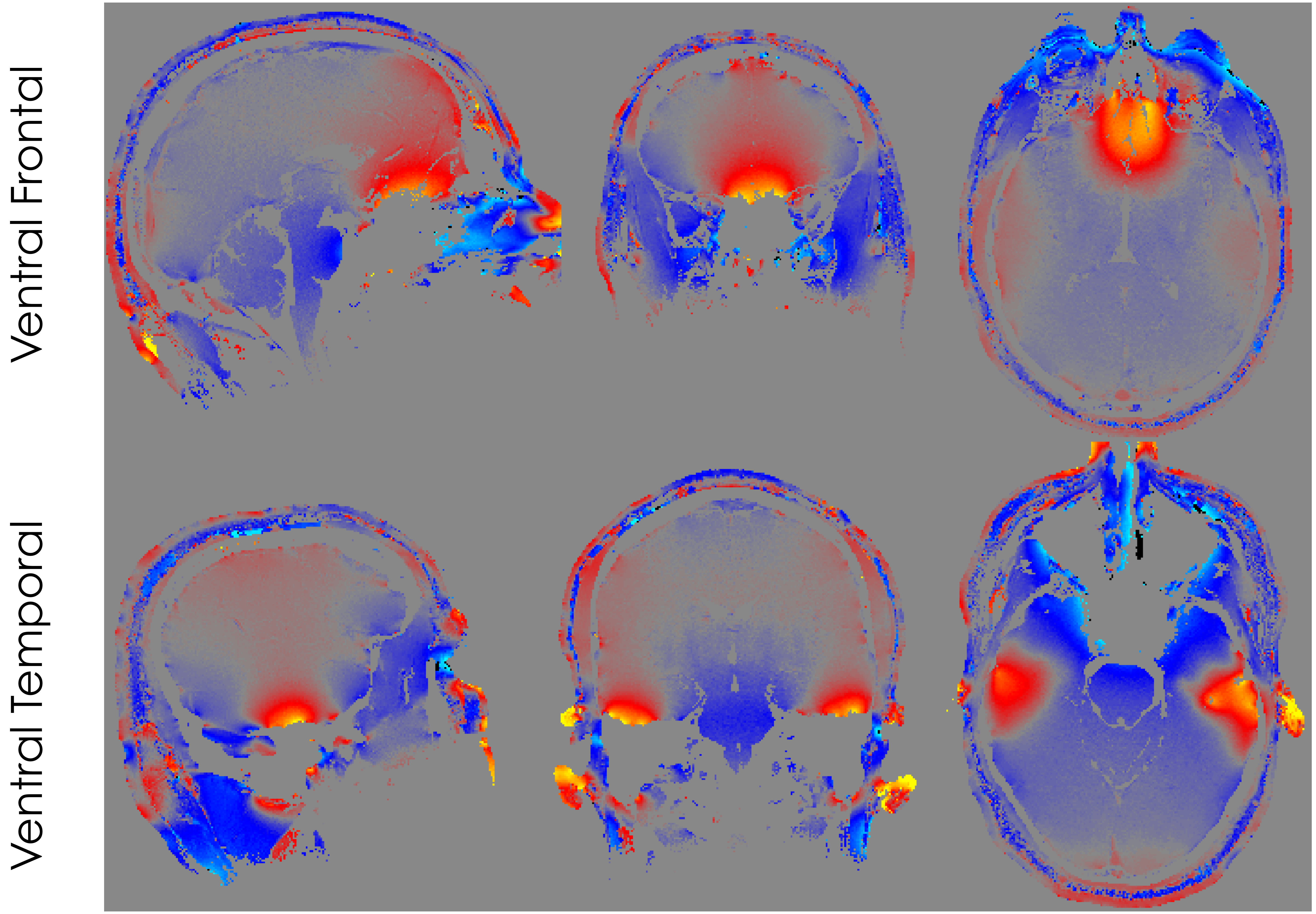

Complex MEMP-RAGE B0 map

B0 inhomogeneity and T2*

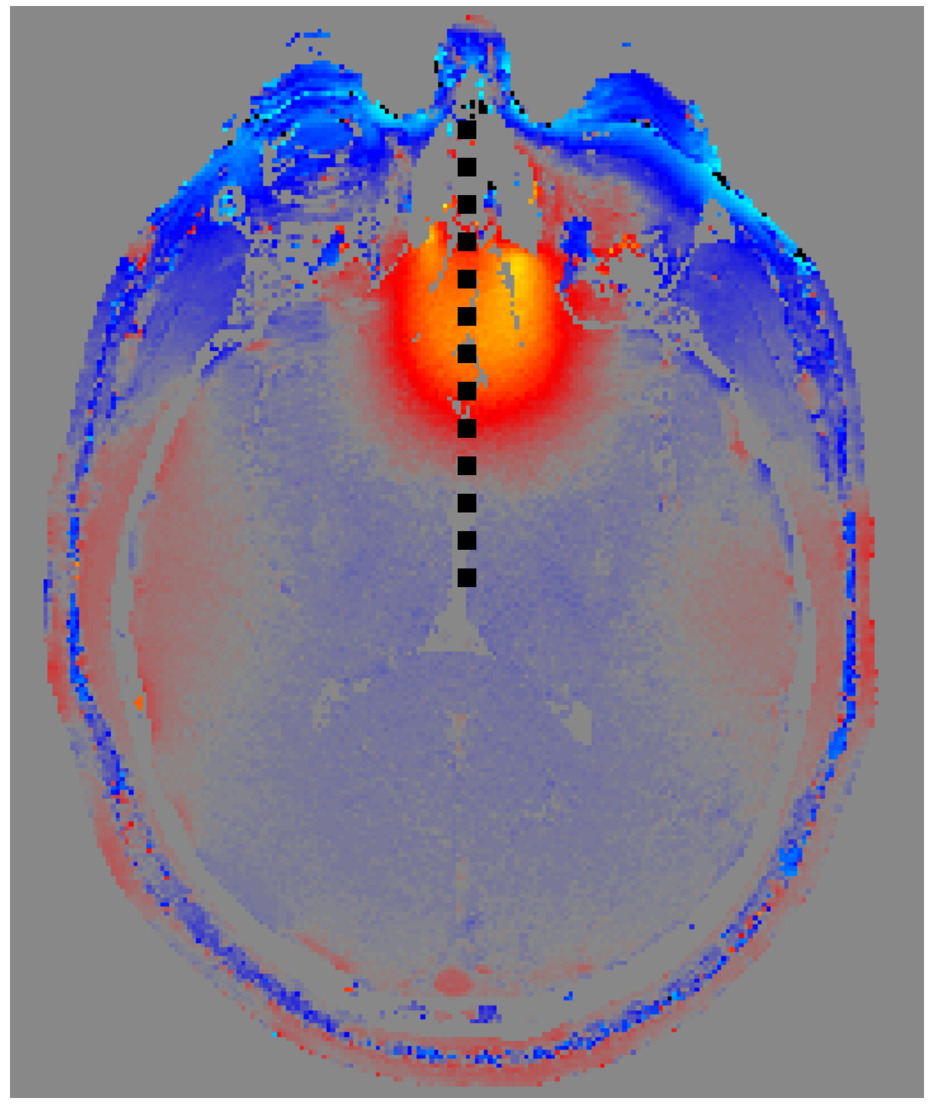

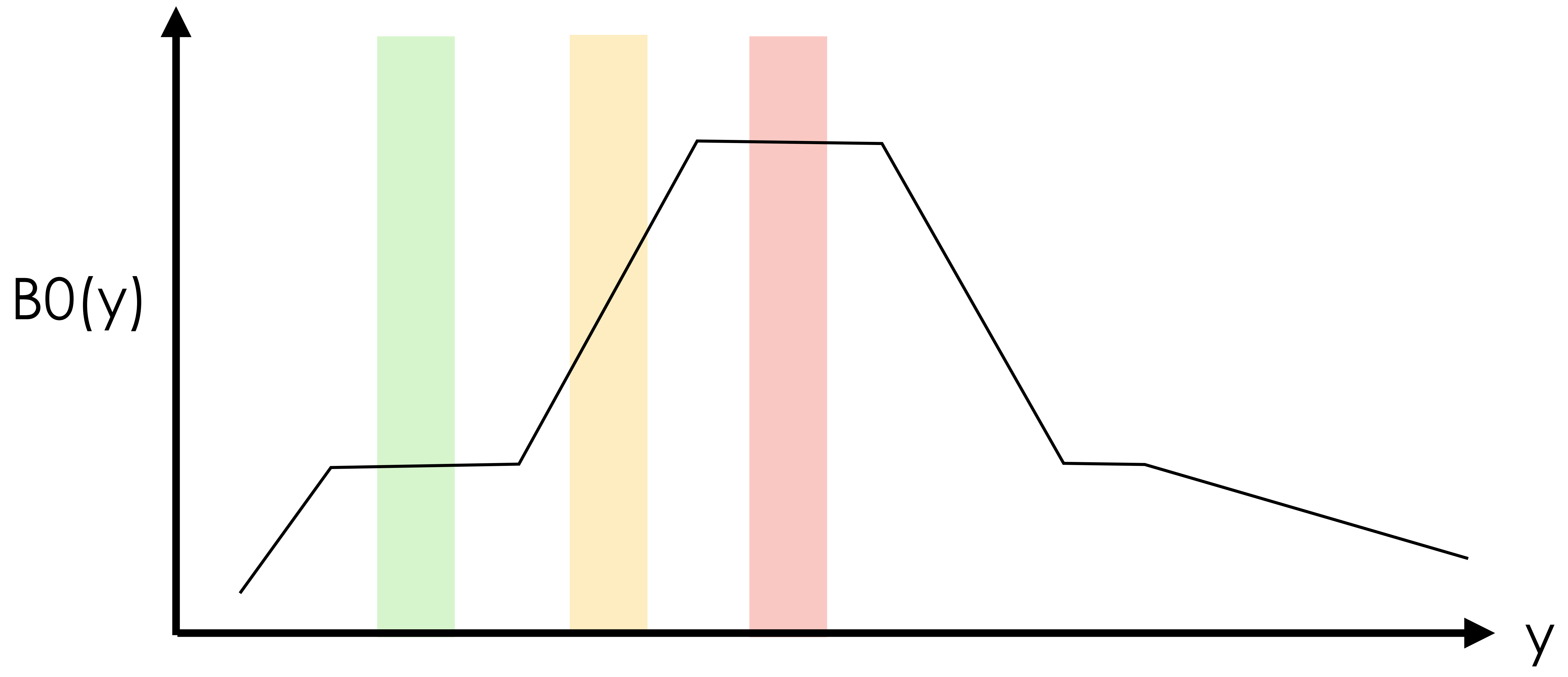

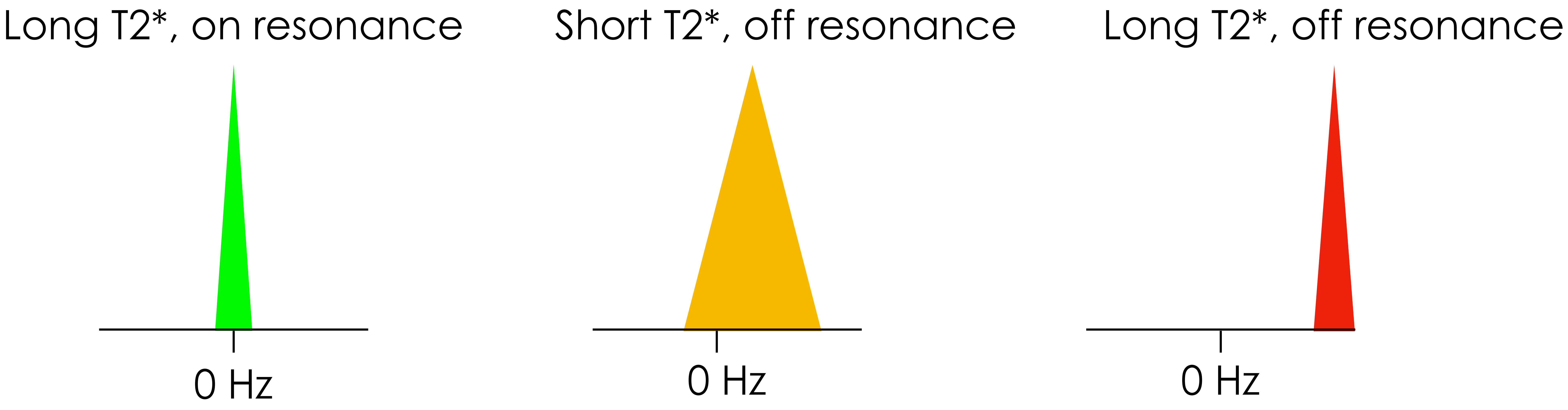

T2* Dropout in GRE-EPI

SE-EPI

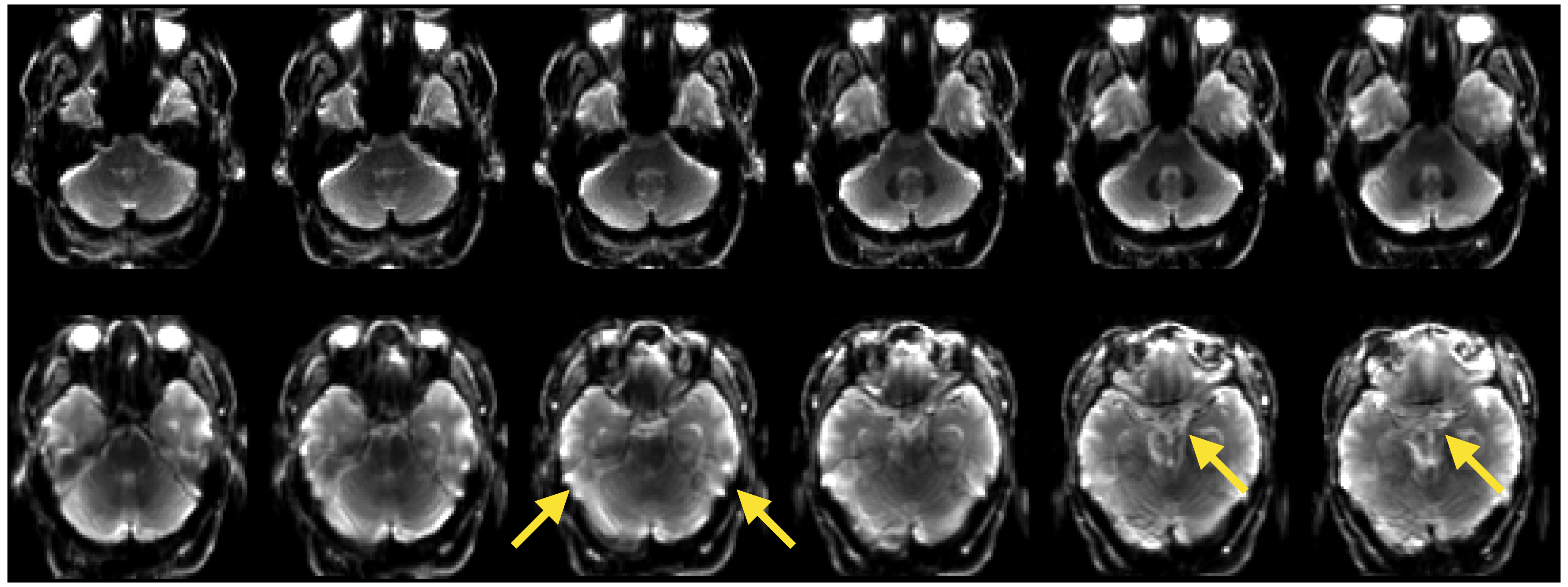

Estimated B0 Field

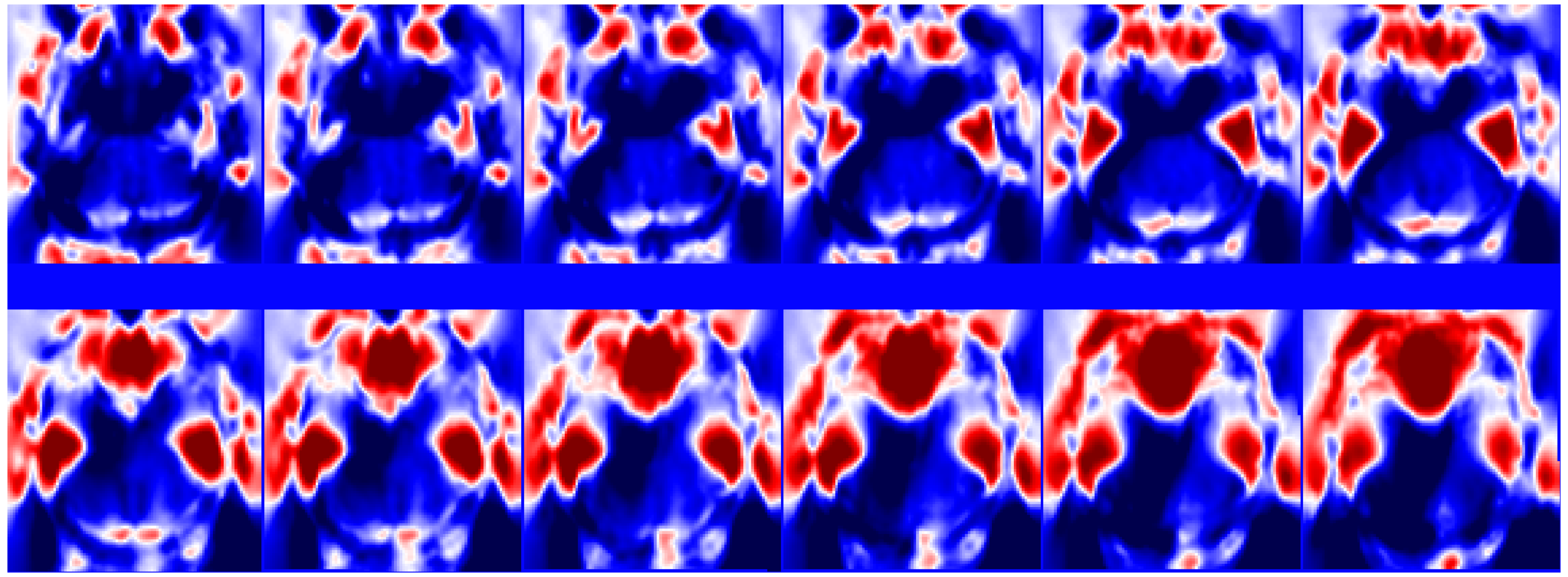

GRE-EPI

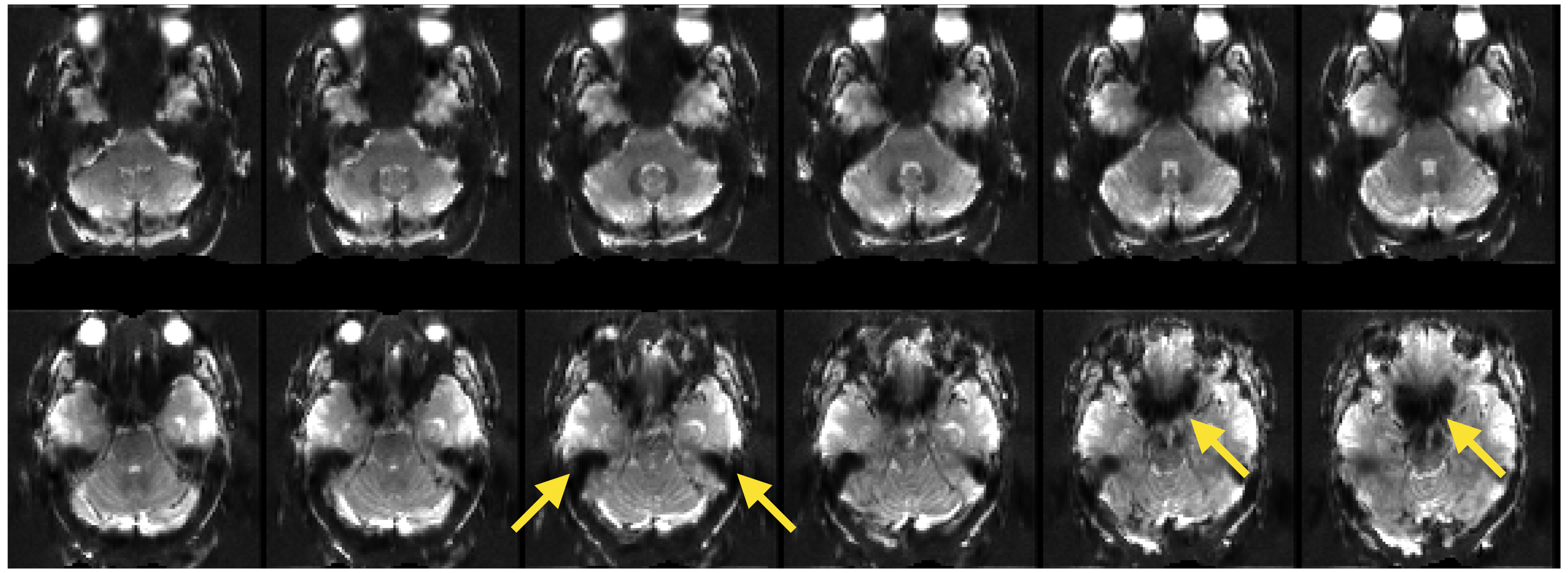

Estimated Dropout

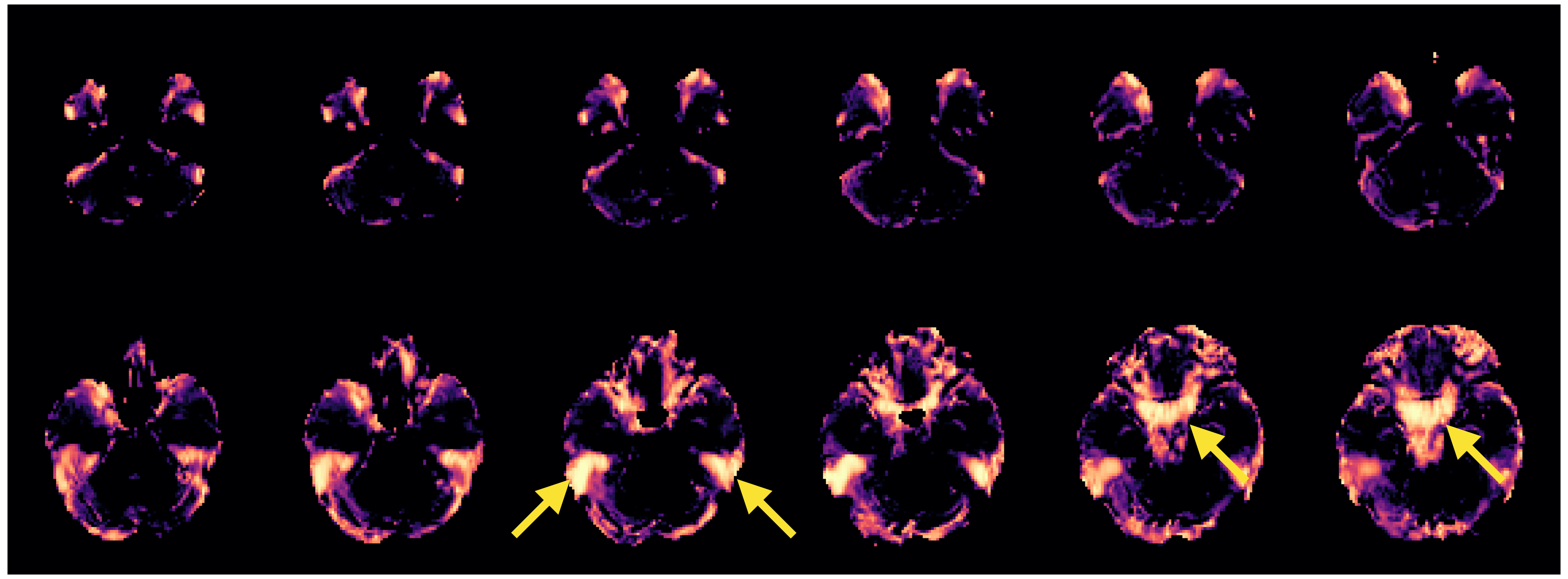

New Concept : Acquisition Bandwidth

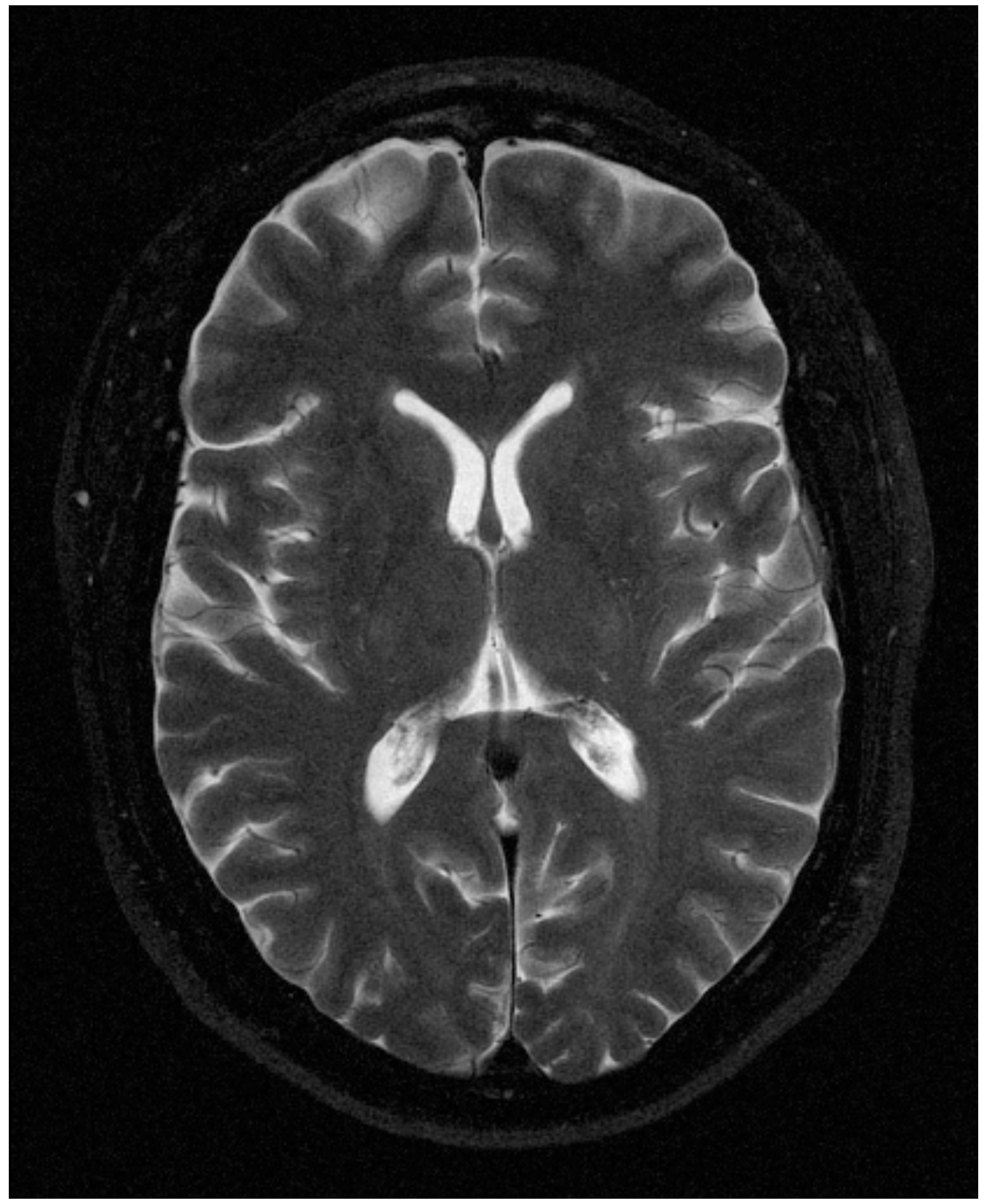

Field of view of image in terms of frequency

$$BW = \gamma G_x FOV_x$$

$$[Hz] = \left[\frac{Hz}{G}\right]\left[\frac{G}{cm}\right][cm]$$

$$B_z = B_0 + G_x x$$

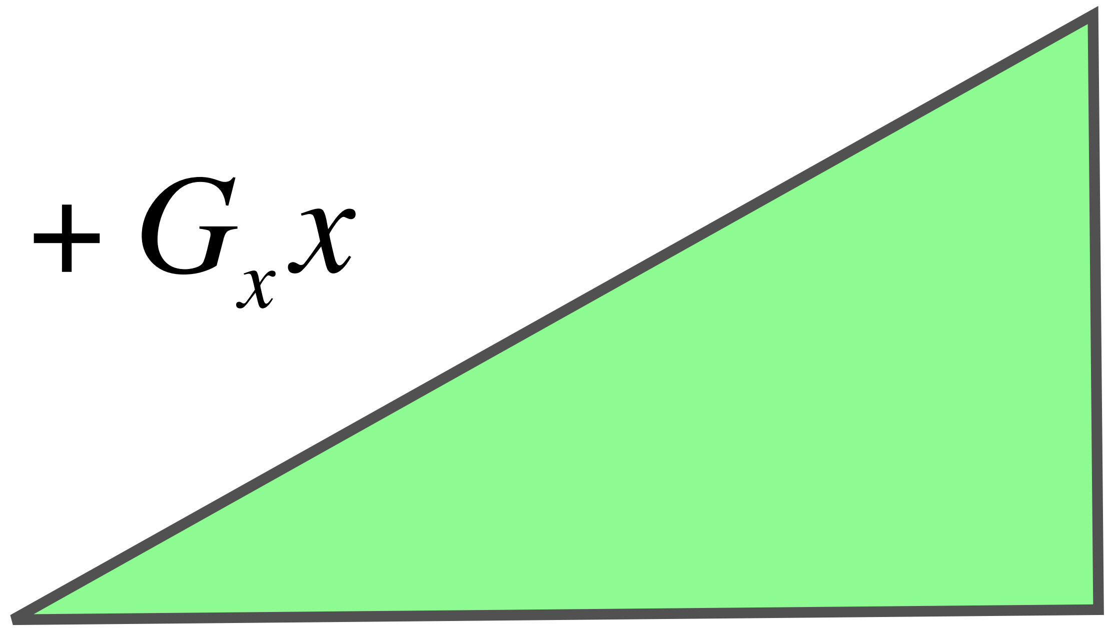

EPI Bandwidths

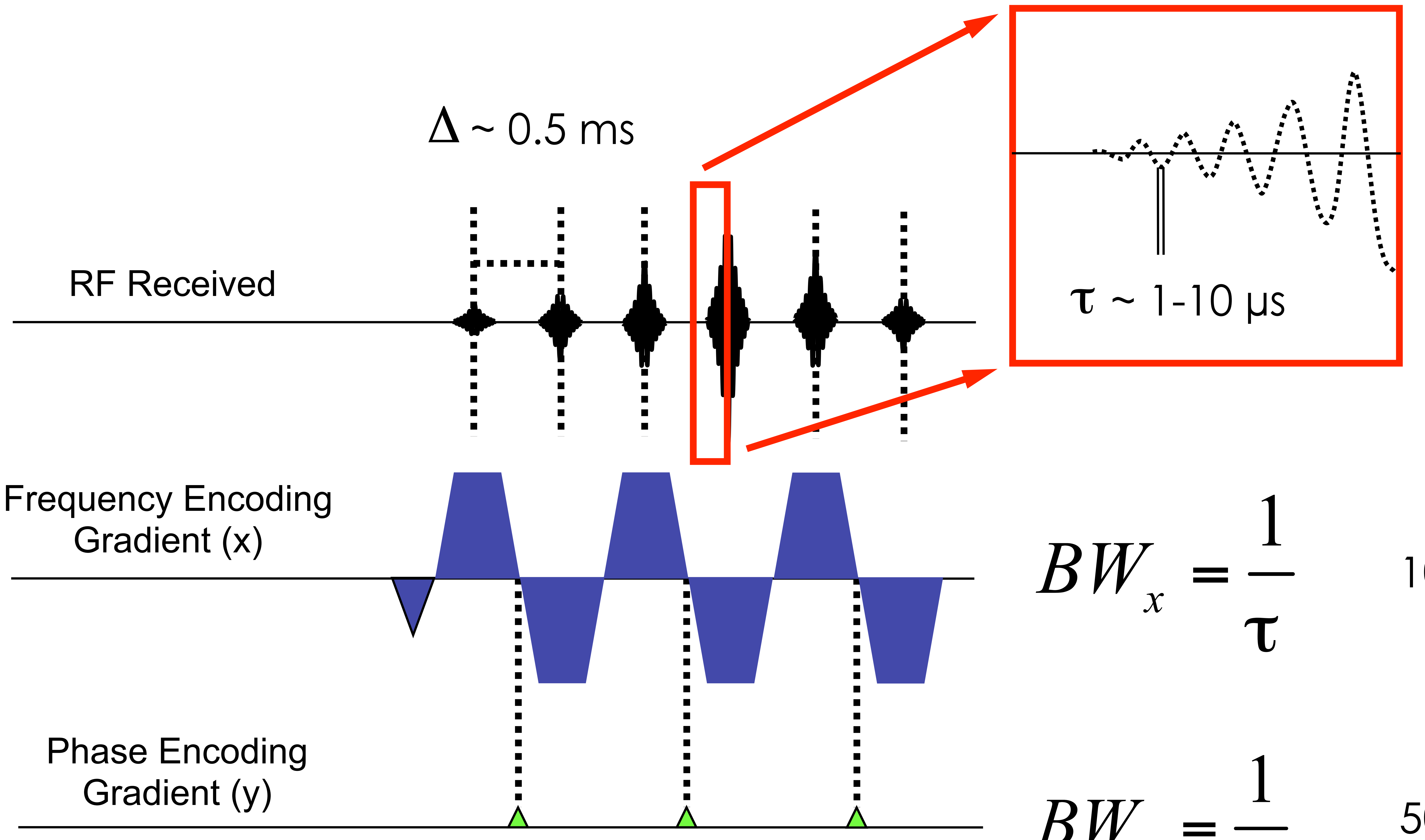

$$BW_x = \frac{1}{\tau}$$

100 kHz - 2 MHz

$$BW_y = \frac{1}{\Delta}$$

500 Hz to 2 KHz

Off-resonance Effects and EPI

B0 inhomogeneities cause resonance frequency to vary within the brain

Frequency Encoding Direction
(High Bandwidth)

AP Phase
Encoding
Displacement

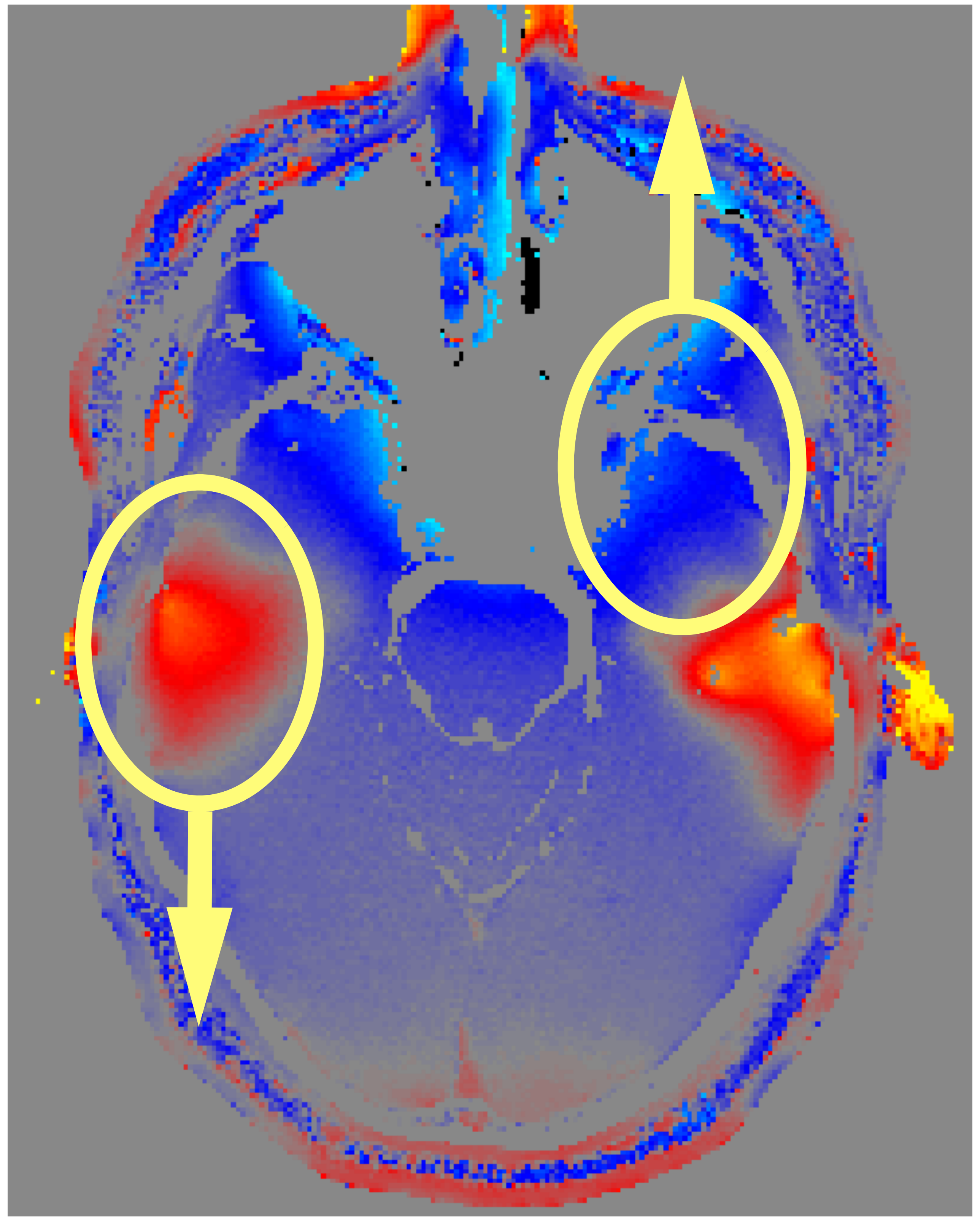

Phase Encoding Direction
(Low Bandwidth)

Voxel displacement primarily in low BW direction (PE)

$$\Delta y = \frac{\gamma \Delta B_0 \cdot \mathrm{FOV_y}}{\mathrm{BW_y}}$$

EPI Geometric Distortion

EPI Geometric Distortion

Effect of Echo Train Length

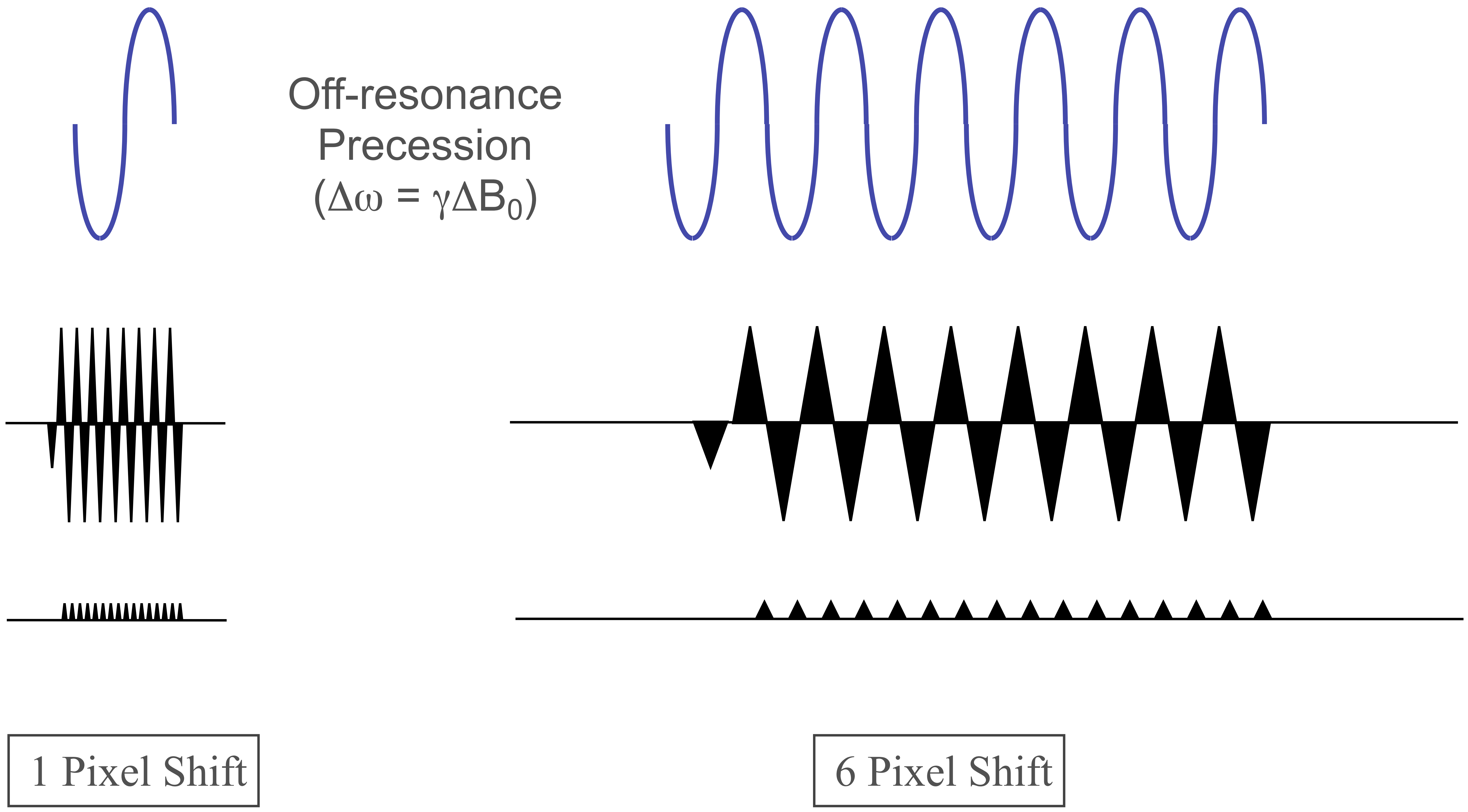

Echo train length and geometric distortion

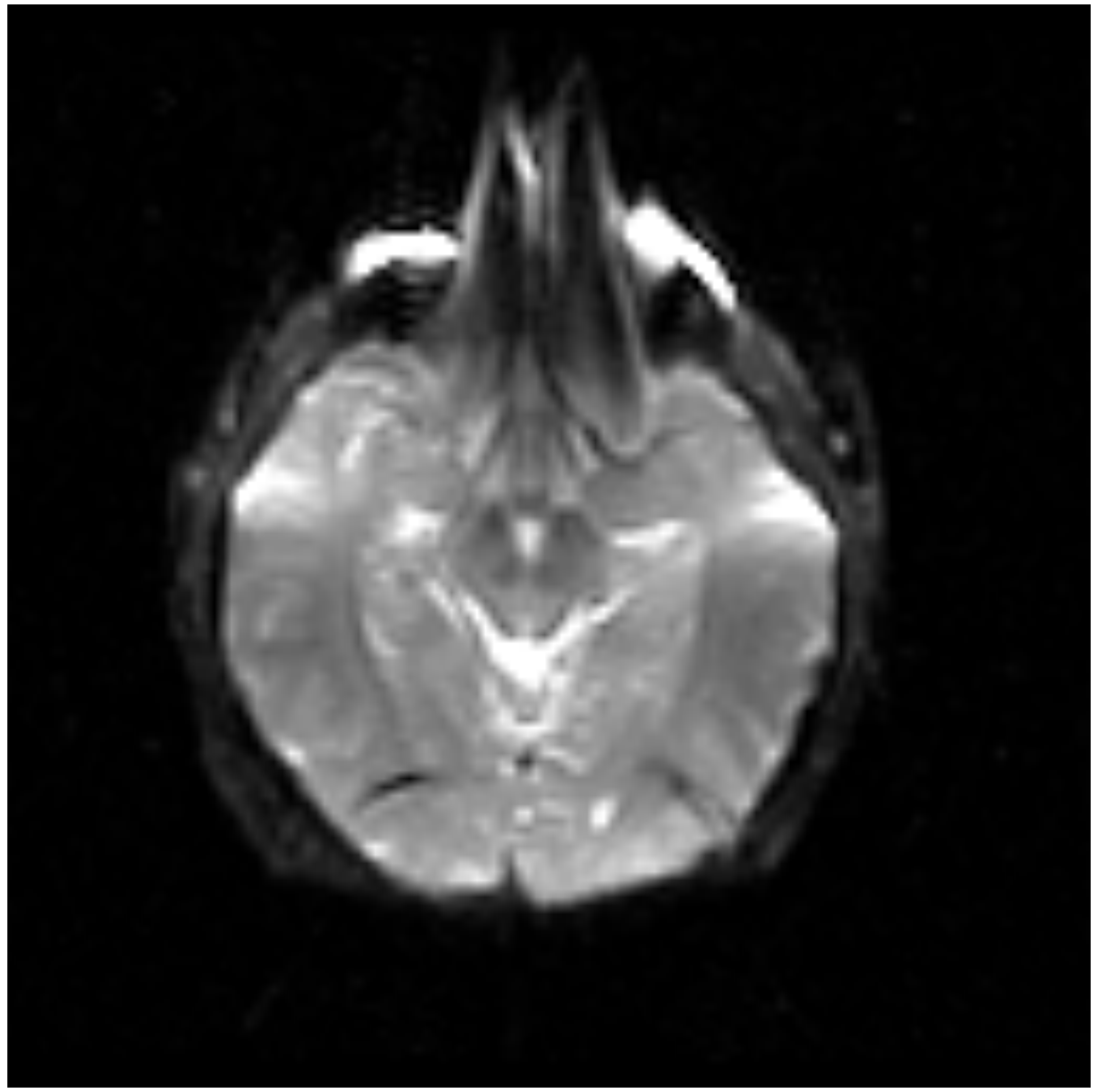

Long echo train

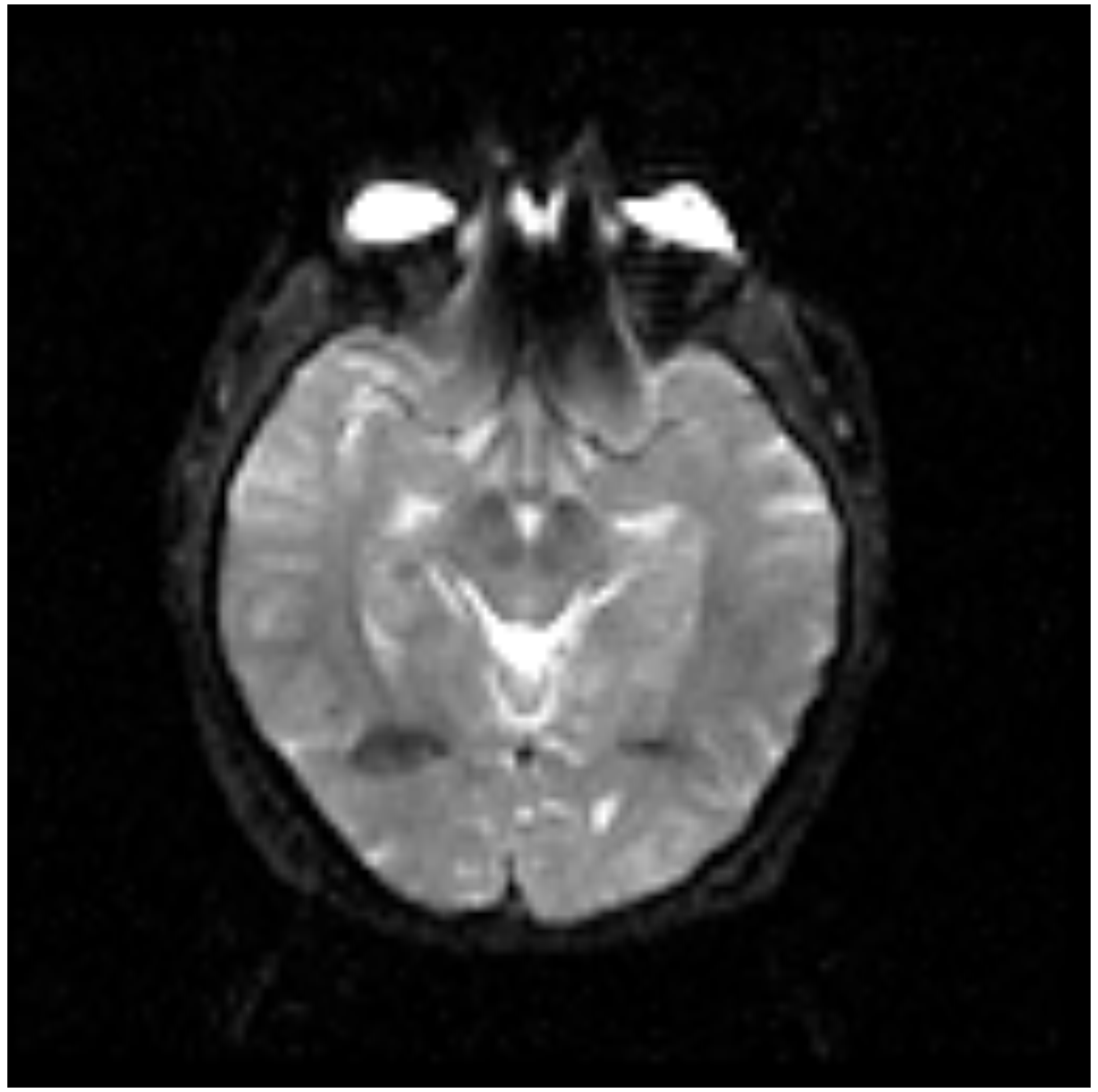

Short echo train

EPI Nyquist Ghosts

Gradient eddy currents and other temporal instabilities cause even and odd EPI echos to advance or delay relative to ideal echo time

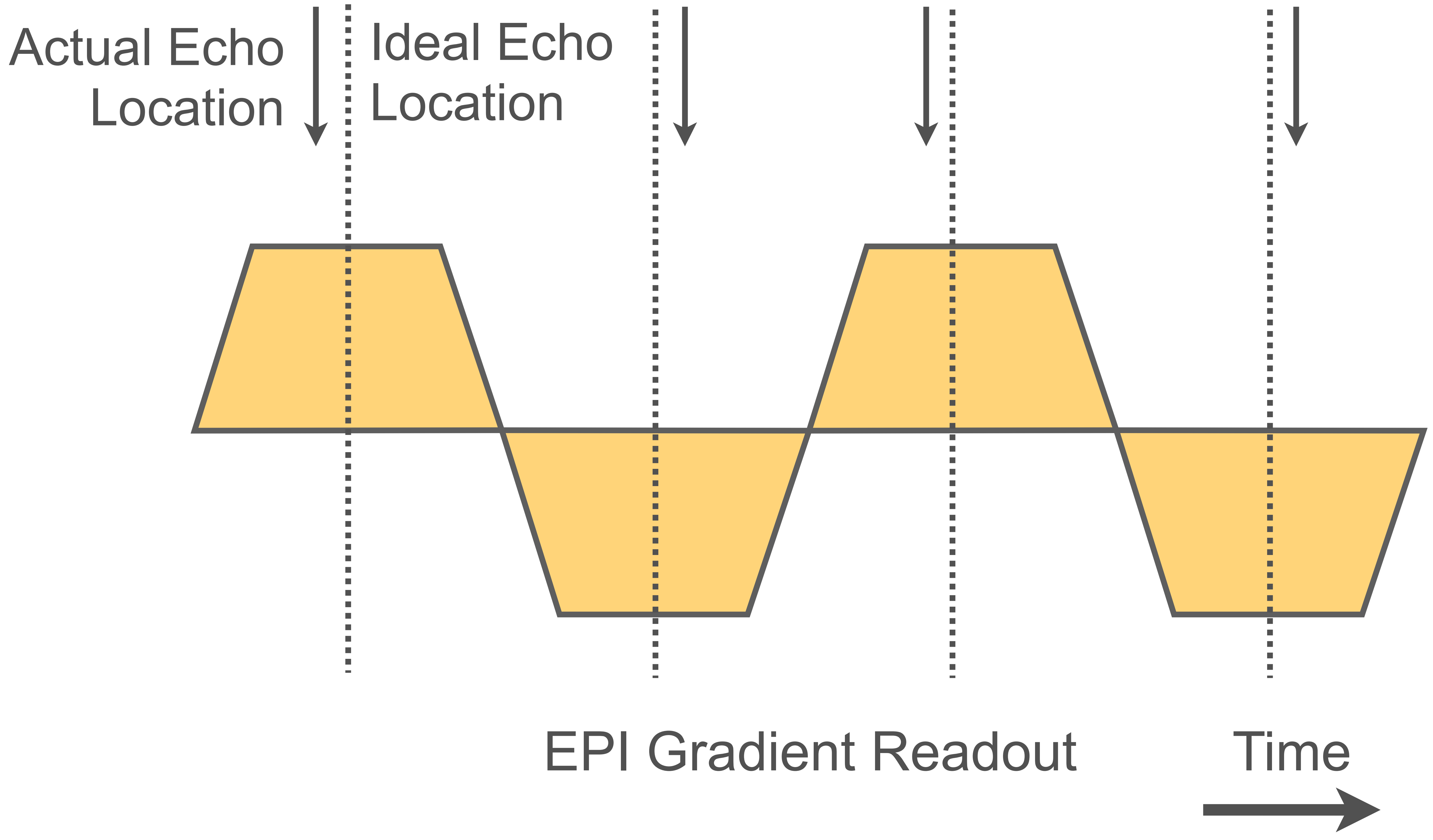

K-space

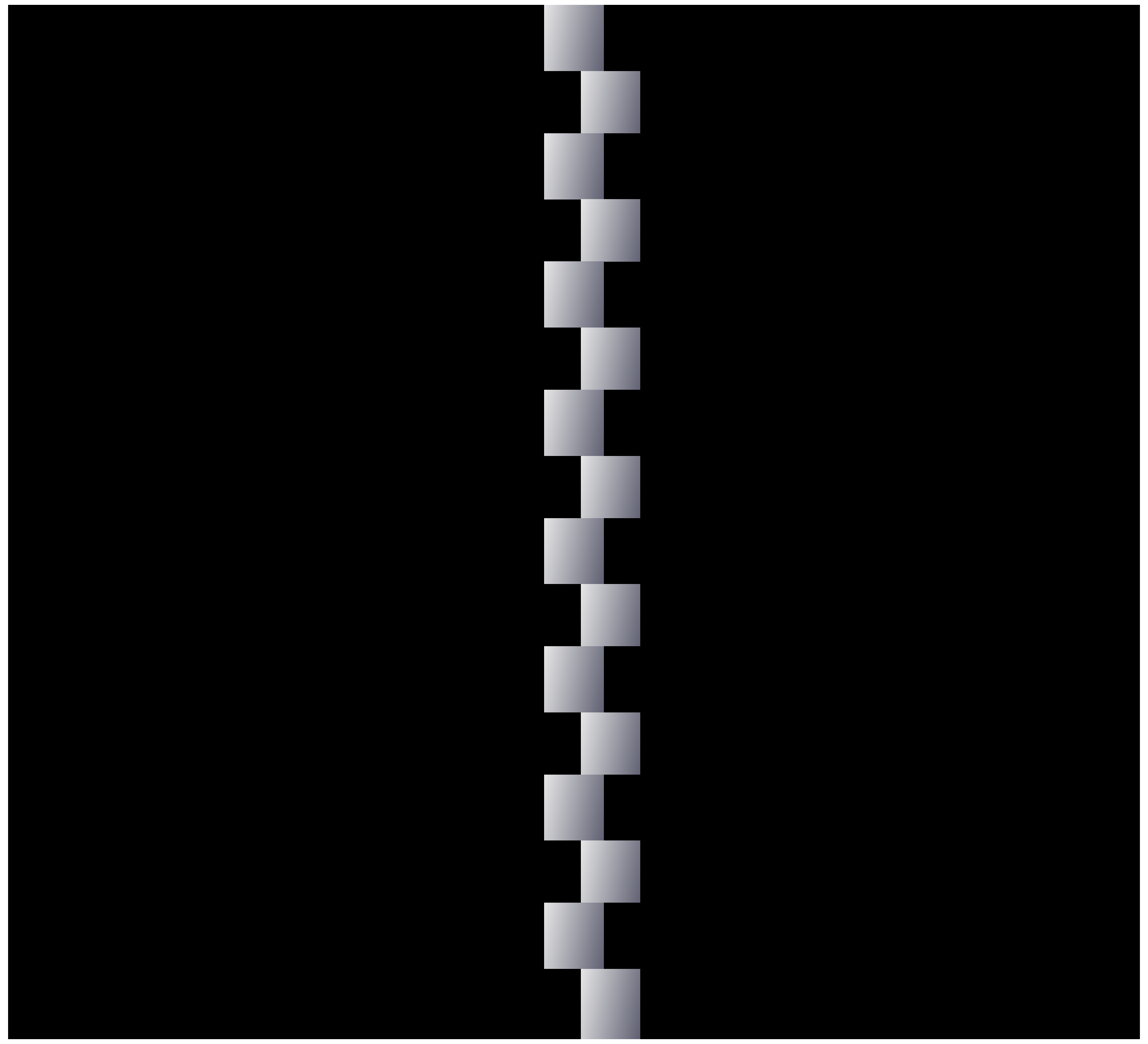

Echo position alternates for each row

Nyquist frequency for row sampling

Nyquist Ghosts

Alternating row echo displacement in k-space results in a ghost of the main image shifted by exactly half the field of view in the phase encoding direction.

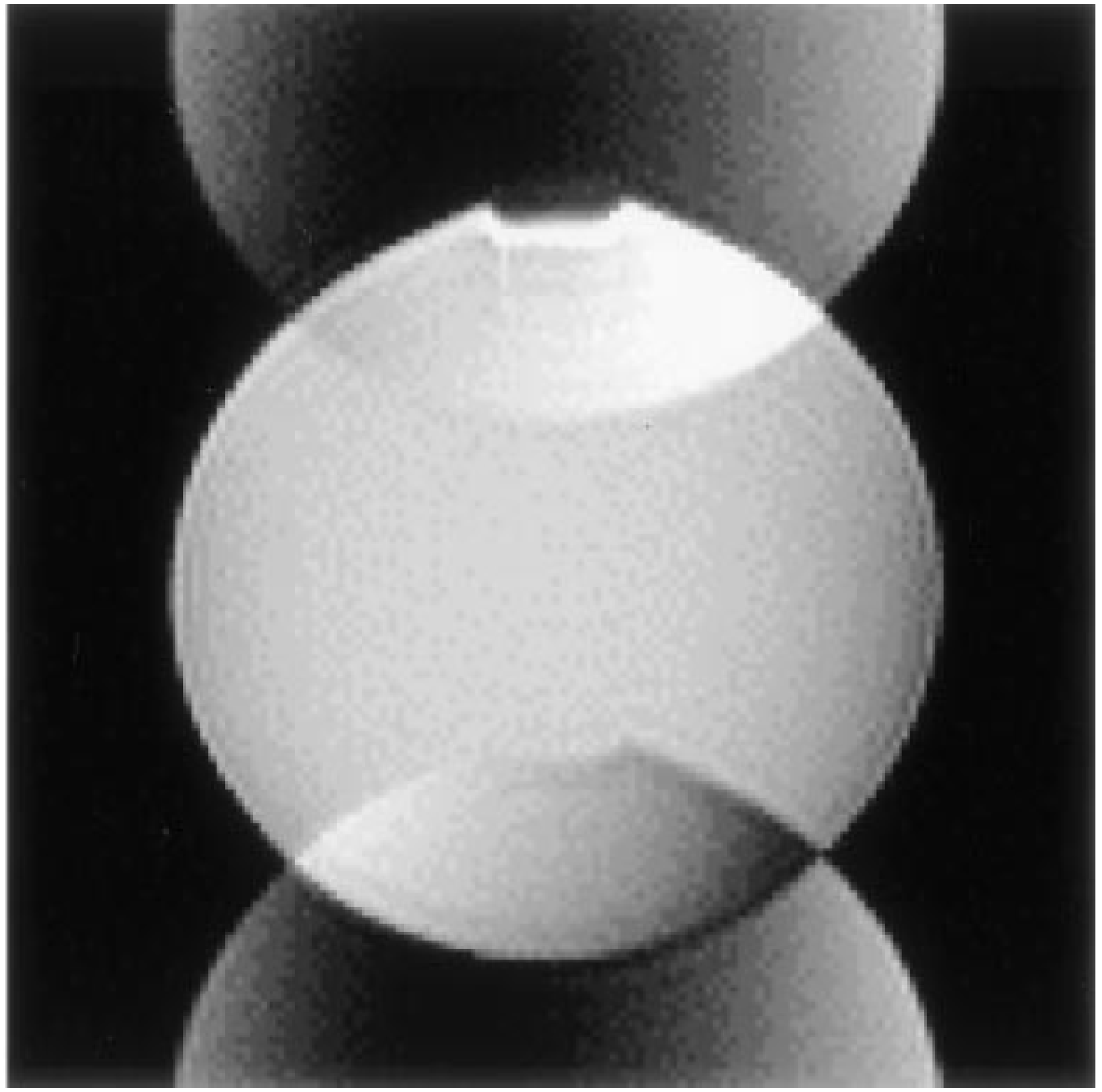

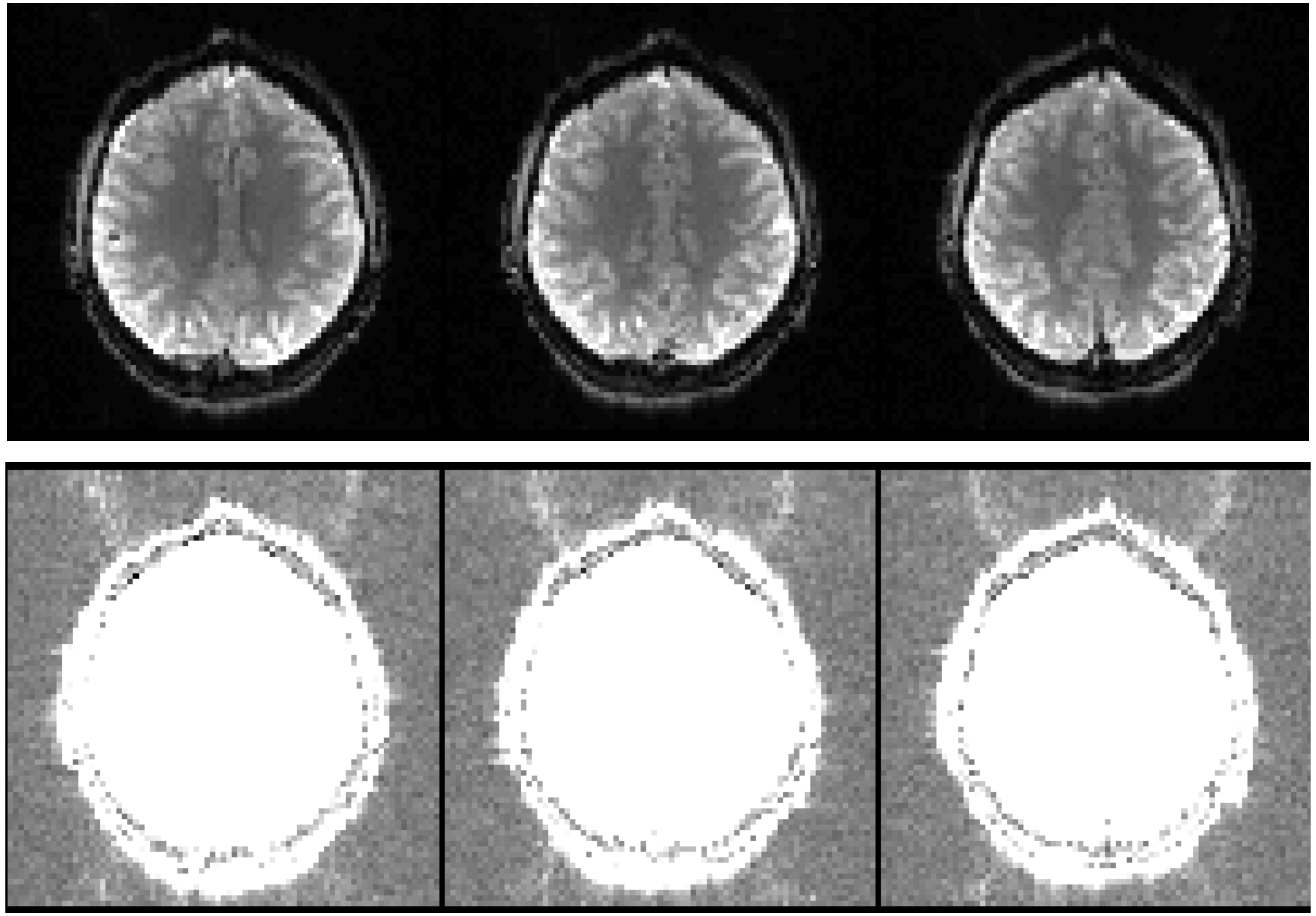

Well-corrected Nyquist ghosting in cooperating participant

Fat-Water Displacement Artifact

Mobile lipid protons resonate at a lower frequency than water protons

When the phase encoding bandwidth is low (EPI) the fat signal displaces significantly

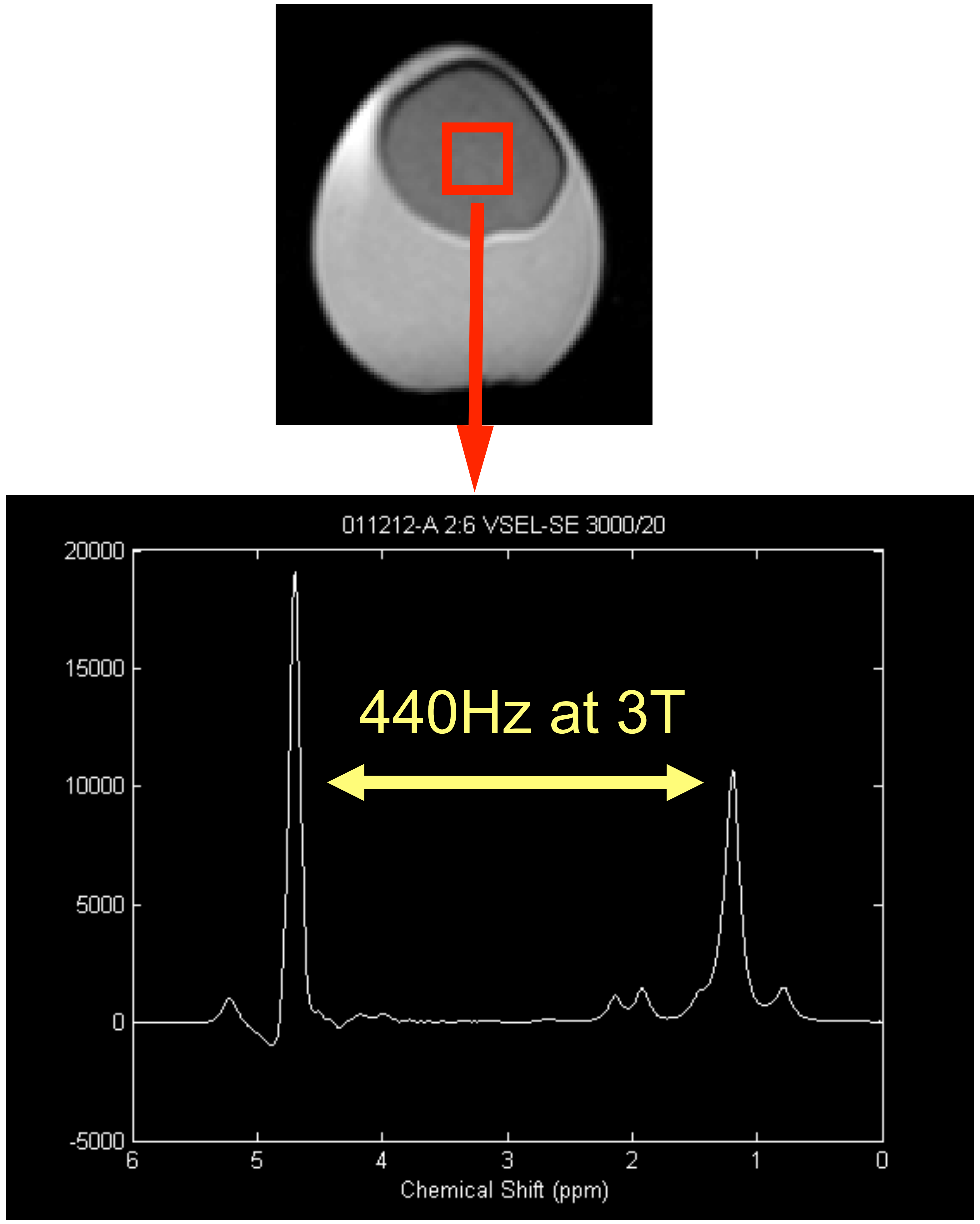

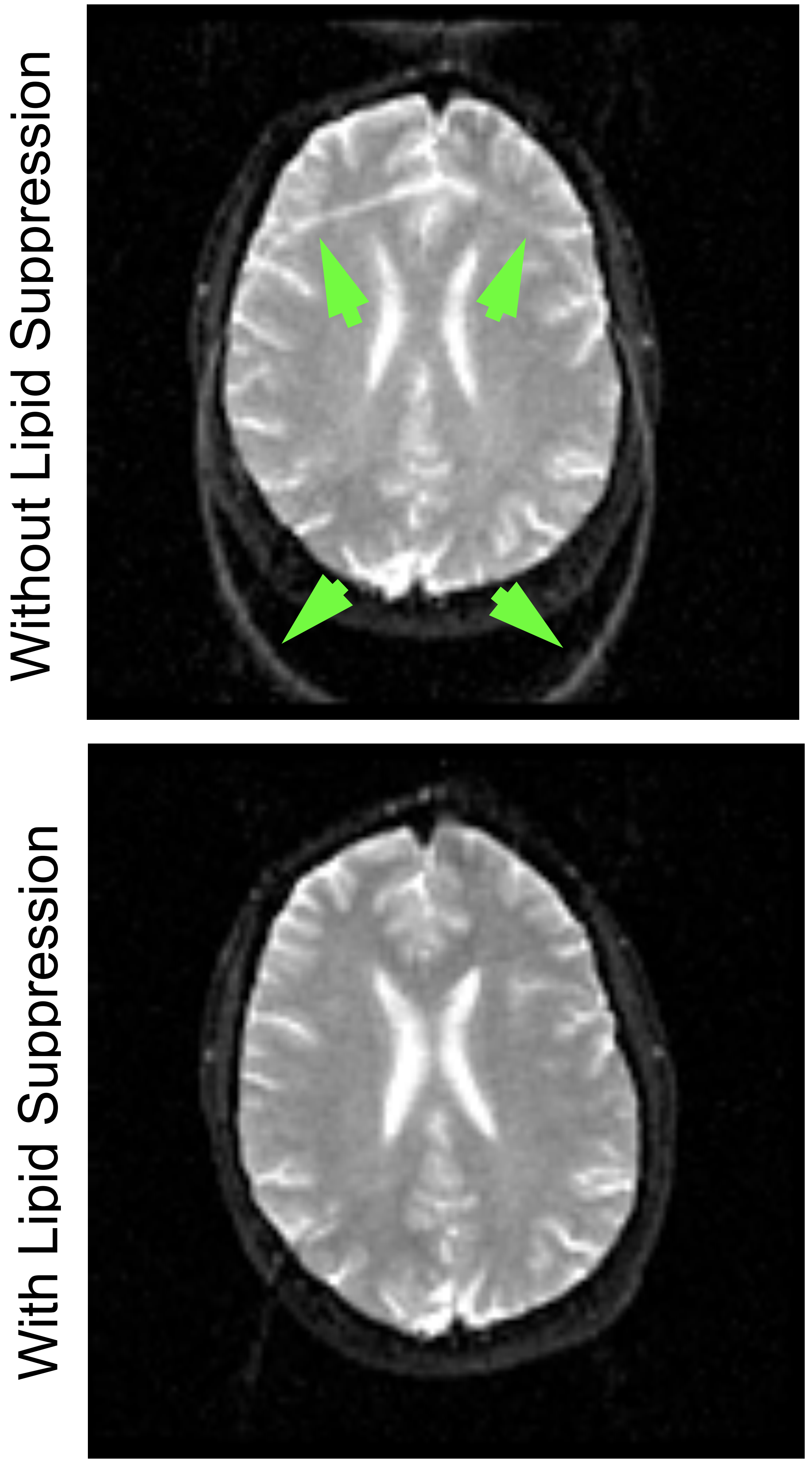

B_1 Inhomogeneity

Spatial inhomogeneity of transmit B1 field (B1+) and receive coil sensitivity

Focus on the latter with body coil transmit at 3T

B_1 Inhomogeneity

Spatial inhomogeneity of transmit B1 field (B1+) and receive coil sensitivity

Focus on the latter with body coil transmit at 3T

Gibbs Ringing

Undersampled k-space

Equivalent to filtering with a boxcar function

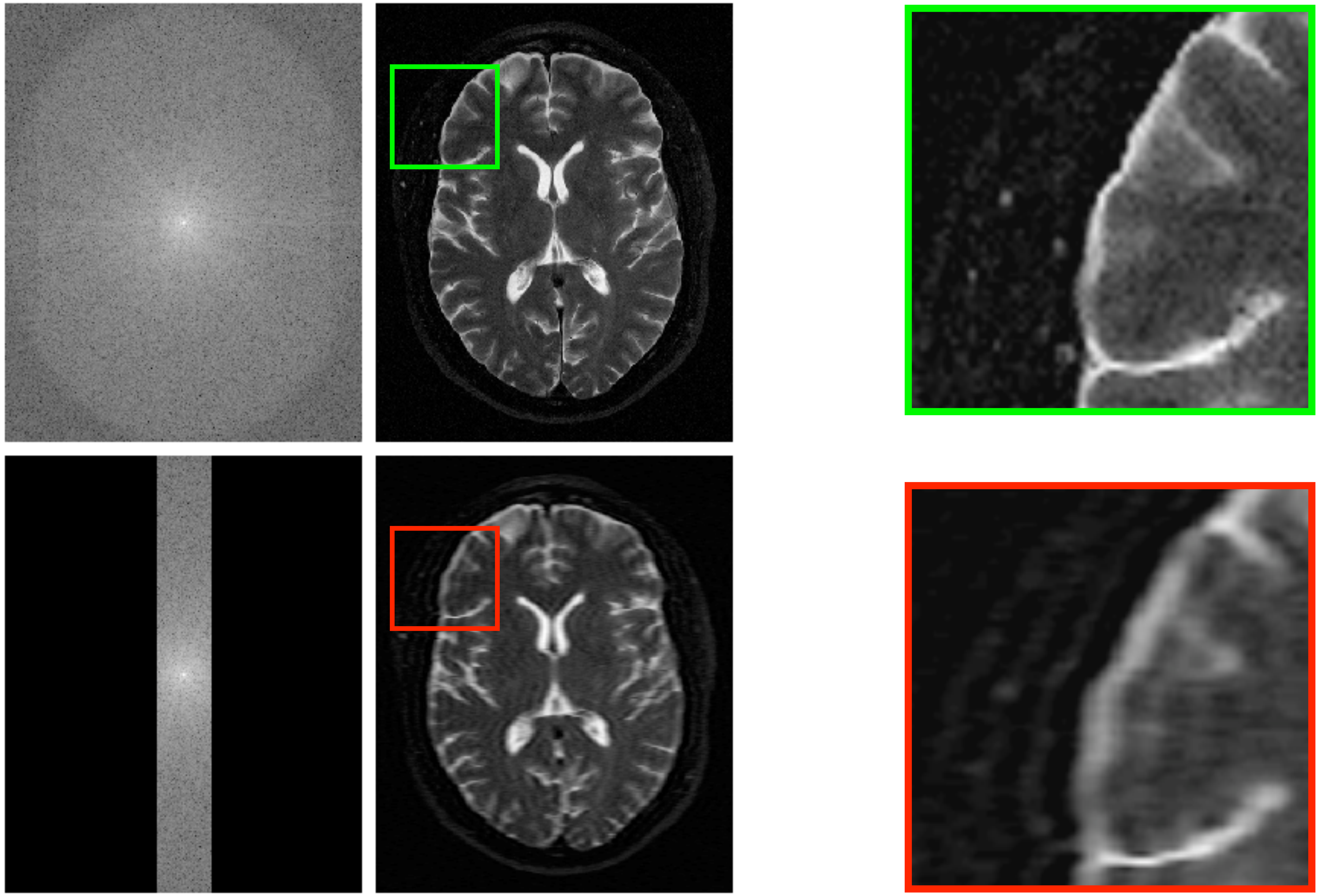

Optimizing MRI

The MRI Tradeoff

Time invested in acquiring data

TIME

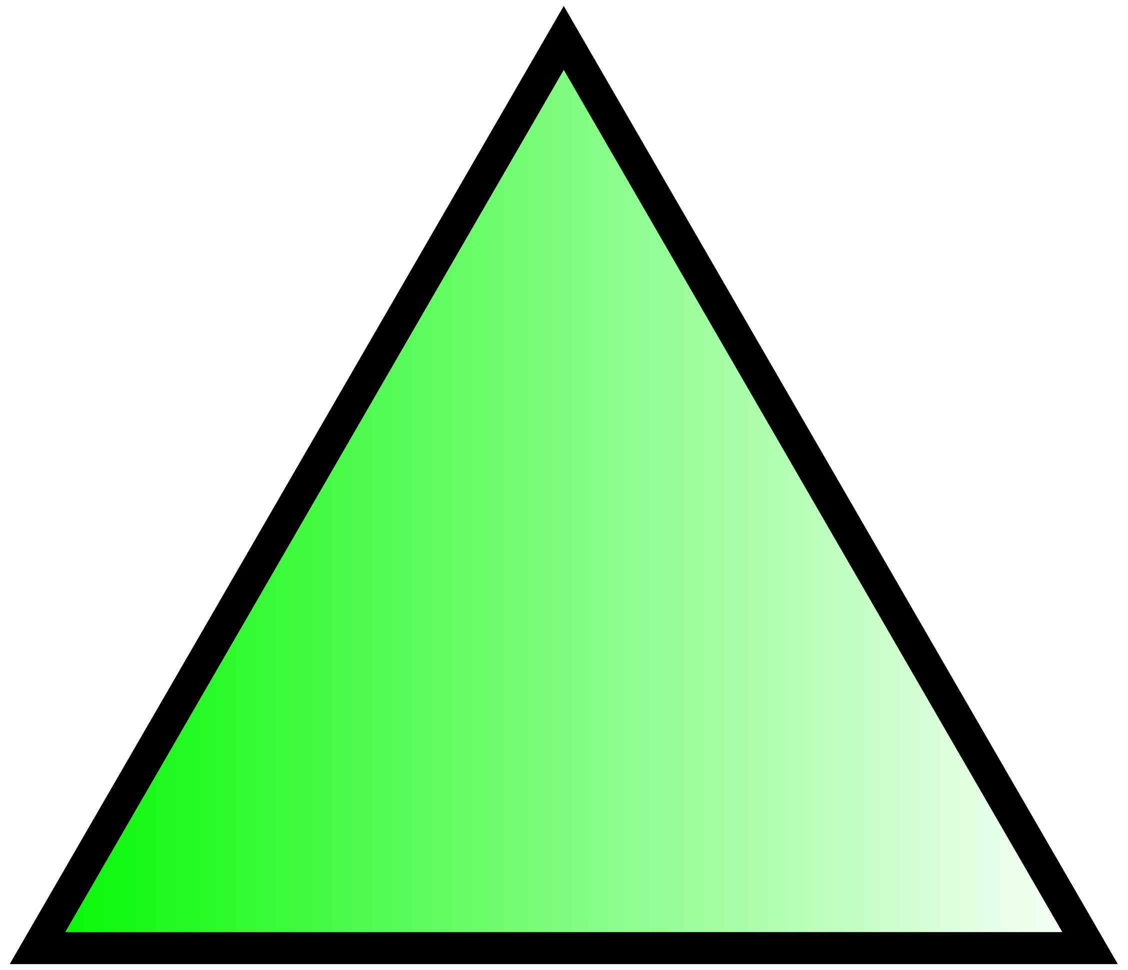

RESOLUTION

SENSITIVITY

Spatial and temporal resolution

SNR and CNR

Magnetic Resonance Microscopy

Clinical MRI	Magnetic Resonance Microscopy	
Human Brain	Mouse Brain	Frog Embryo

Human Brain

Mouse Brain

Frog Embryo

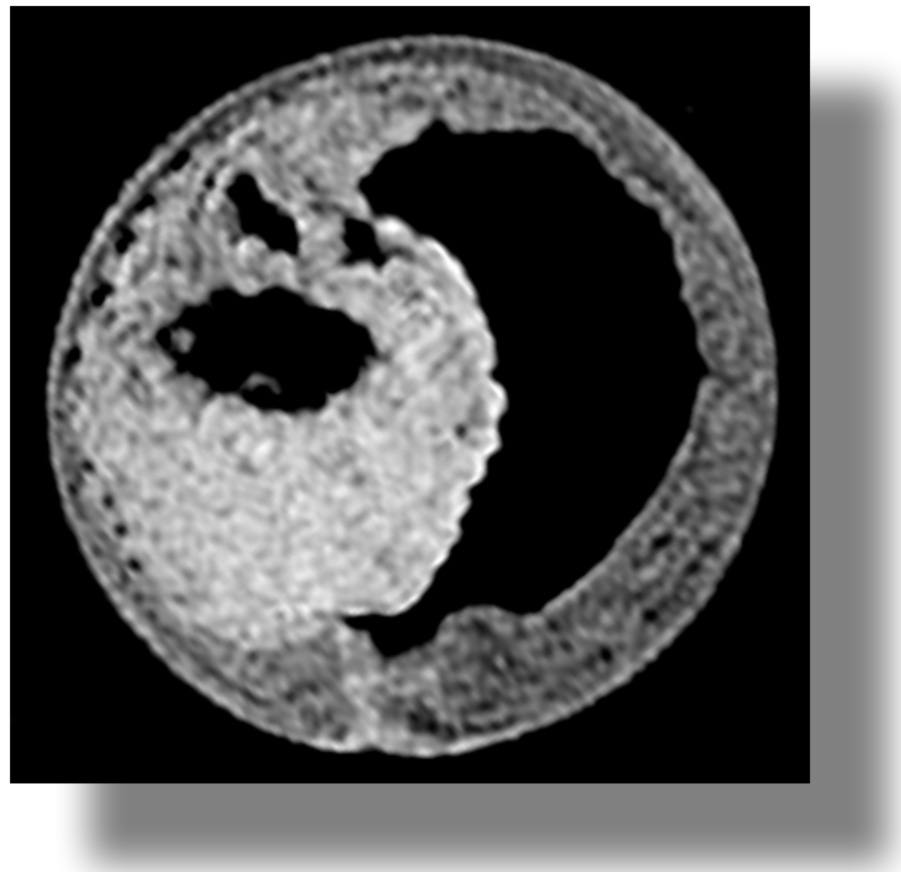

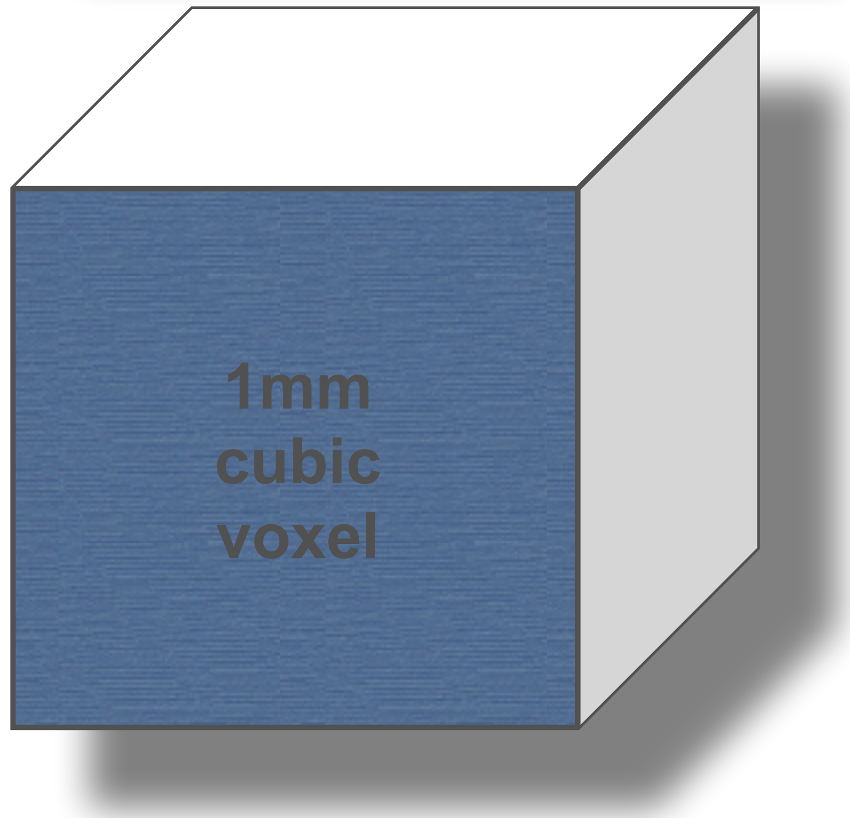

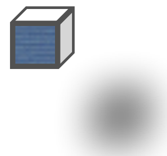

75μm cubic voxel

16μm cubic voxel

3×10^{19} water molecules/voxel	1×10^{16}	1×10^{14}
7×10^{14} detectable spins	9×10^{11}	1×10^{10}

Limits to MRM Resolution

Fundamental	Technical
Diffusion	SNR
T2 relaxation	Total Imaging Time
Susceptibility	Hardware

Ultimate Resolution Limits of MRI

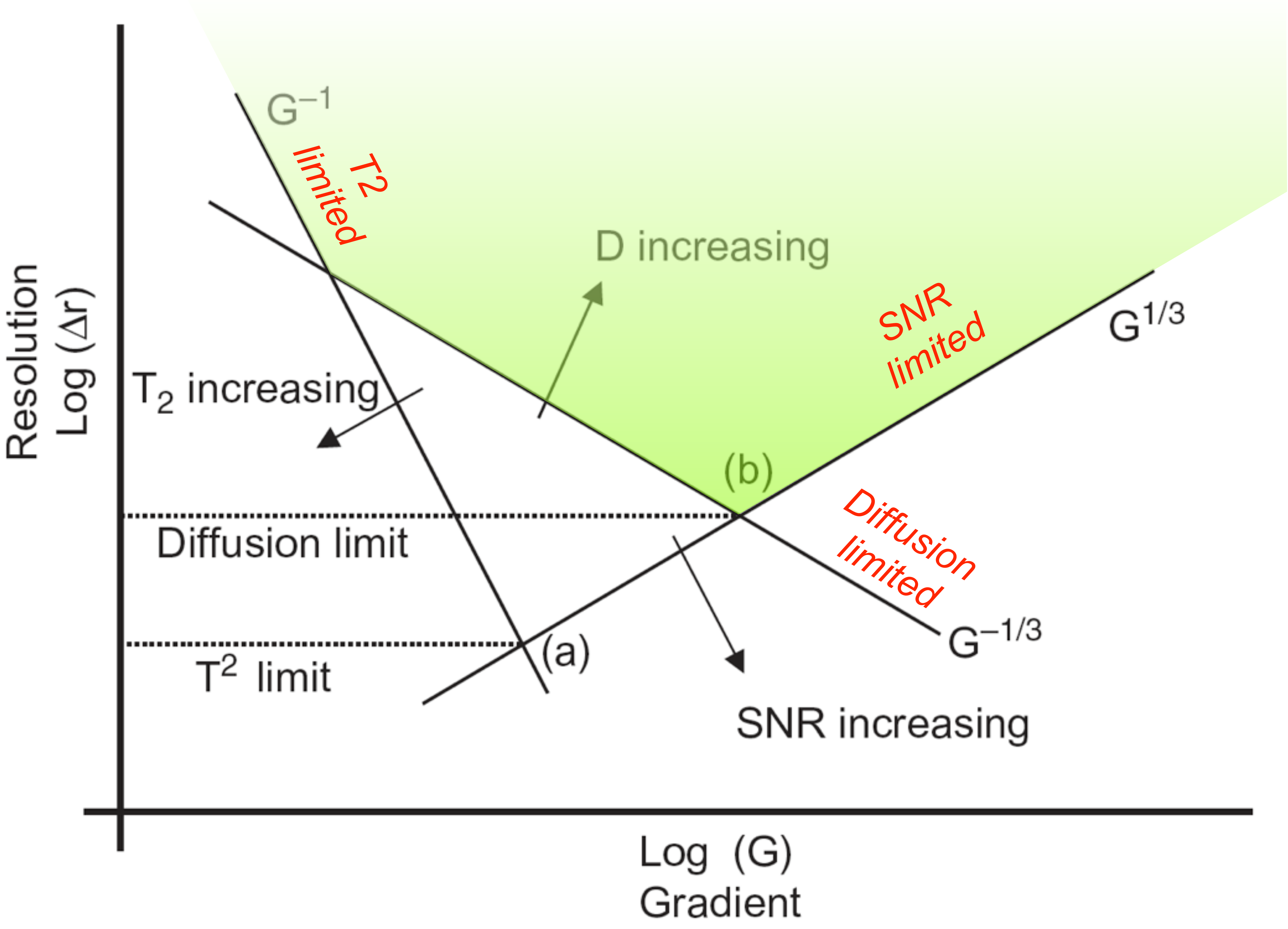

Modified from: Glover and Mansfield Rep Prog Phys 2002;65:1489.

Voxel size and SNR

Total signal from a voxel is proportional to the voxel volume:

$$\frac{S}{N} \propto \Delta x^3 \sqrt{N_{av}}$$

$$N_{av} \propto \frac{1}{\Delta x^6}$$

For a constant SNR, total imaging time has an inverse sixth power relation to voxel dimension!

Frequency Encoding Bandwidth and SNR

SNR is proportional to the square-root of the total digitizer acquisition time
Compare with SNR proportional to the square root of the number of signal averages

$$\frac{S}{N} \propto \sqrt{T_{aq}} = \sqrt{N_x \Delta t} = \sqrt{\frac{N_x}{BW}}$$

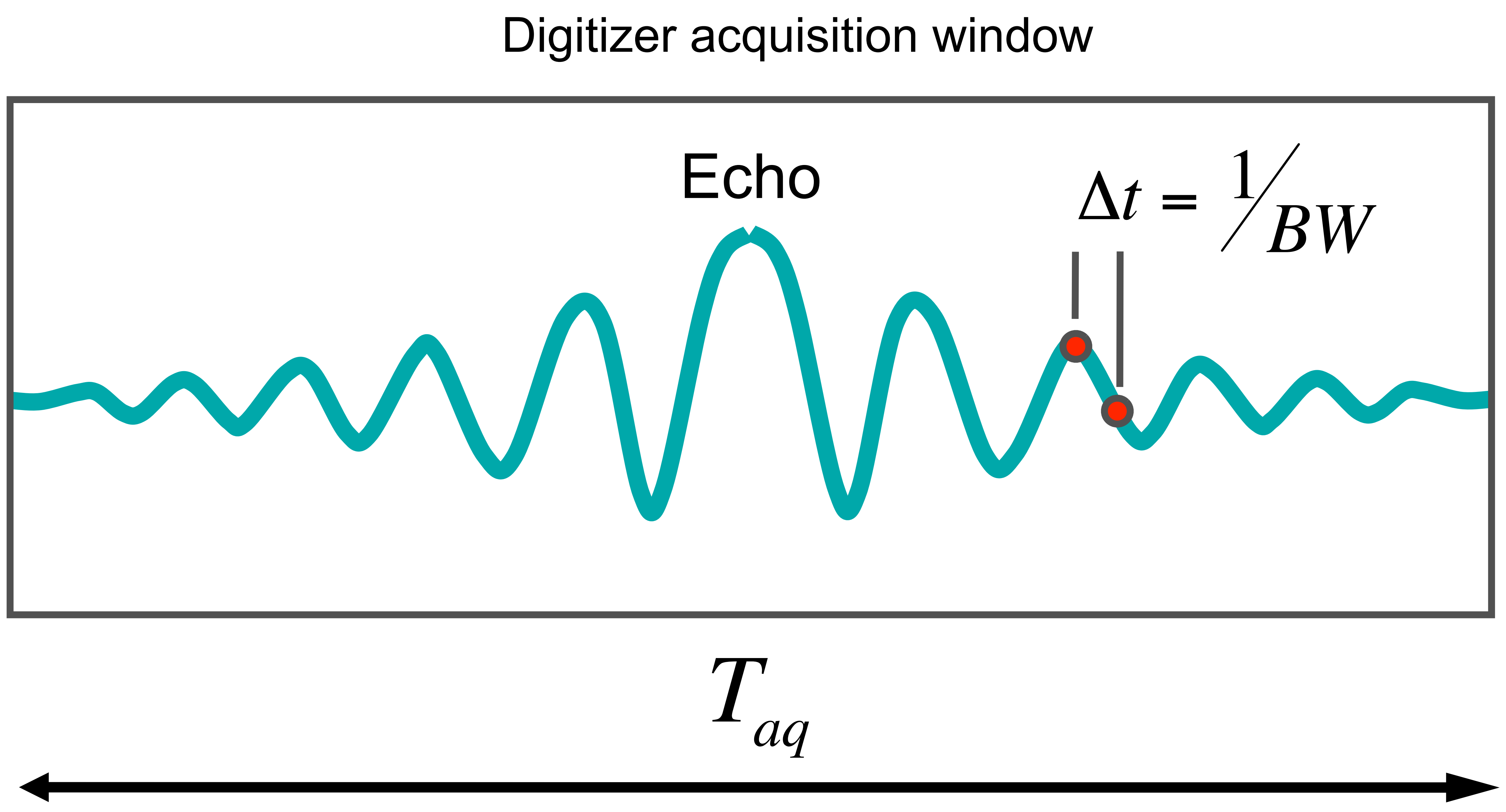

Optimization Considerations

- Design imaging protocol around science question
- Optimize for target brain regions if possible
- Is high spatial resolution really required?
    - Huge SNR penalty for reducing voxel dimensions
- Is high temporal resolution important
    - BOLD hemodynamic response timing
    - Temporal SNR efficiency
    - Physiological denoising

Accelerating MRI

Receive Coil Arrays

Array of small coils with minimal mutual inductance and independent signal reception from each coil

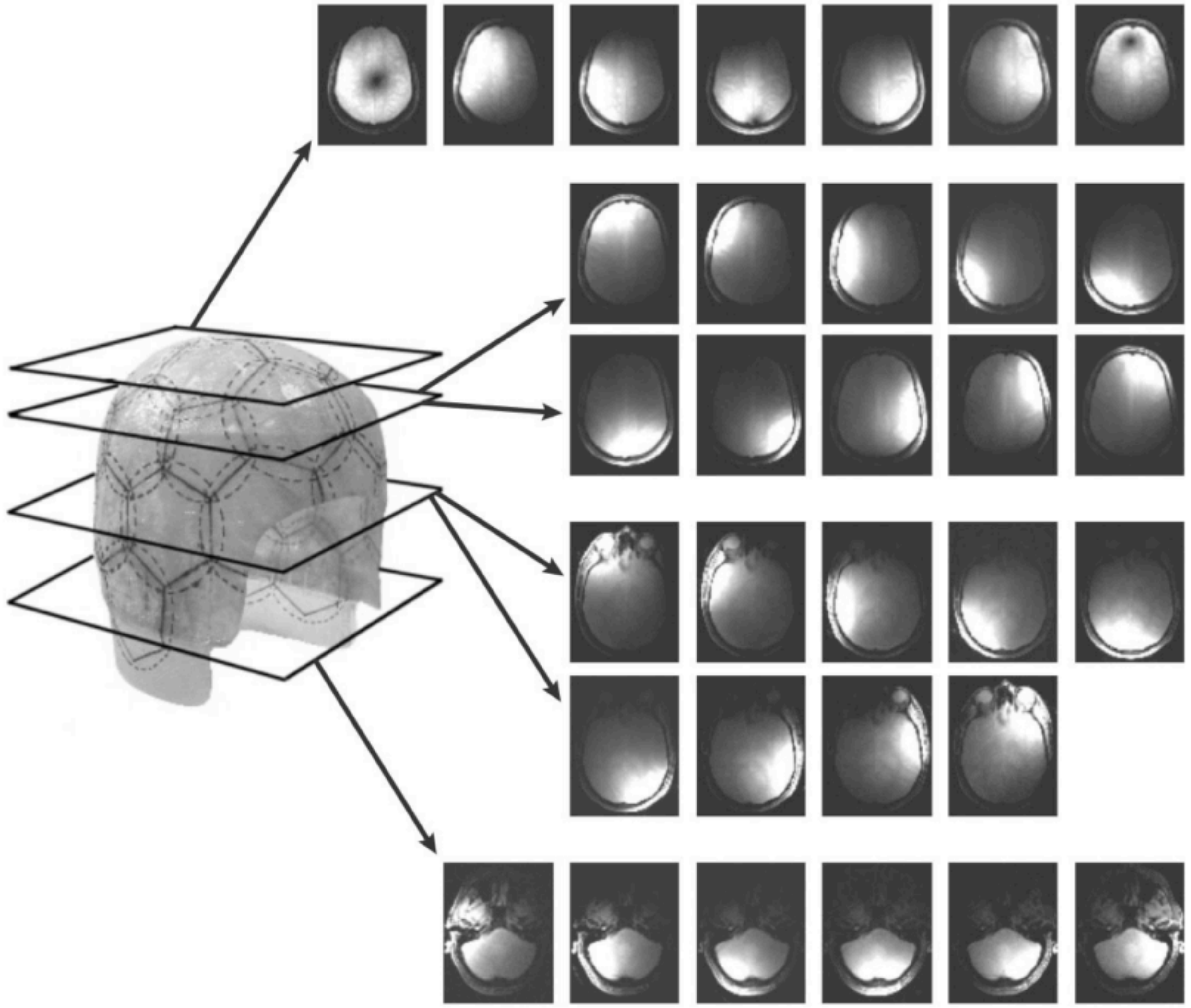

Wiggins, G. C., Triantafyllou, C., Potthast, A., Reykowski, A., Nittka, M., & Wald, L. L. (2006). 32-channel 3 Tesla receive-only phased-array head coil with soccer-ball element geometry. *Magnetic Resonance in Medicine: Official Journal of the Society of Magnetic Resonance in Medicine / Society of Magnetic Resonance in Medicine*, *56*(1), 216–223. https://doi.org/10.1002/mrm.20925

Undersampled k-space and fold-over

Full k-space

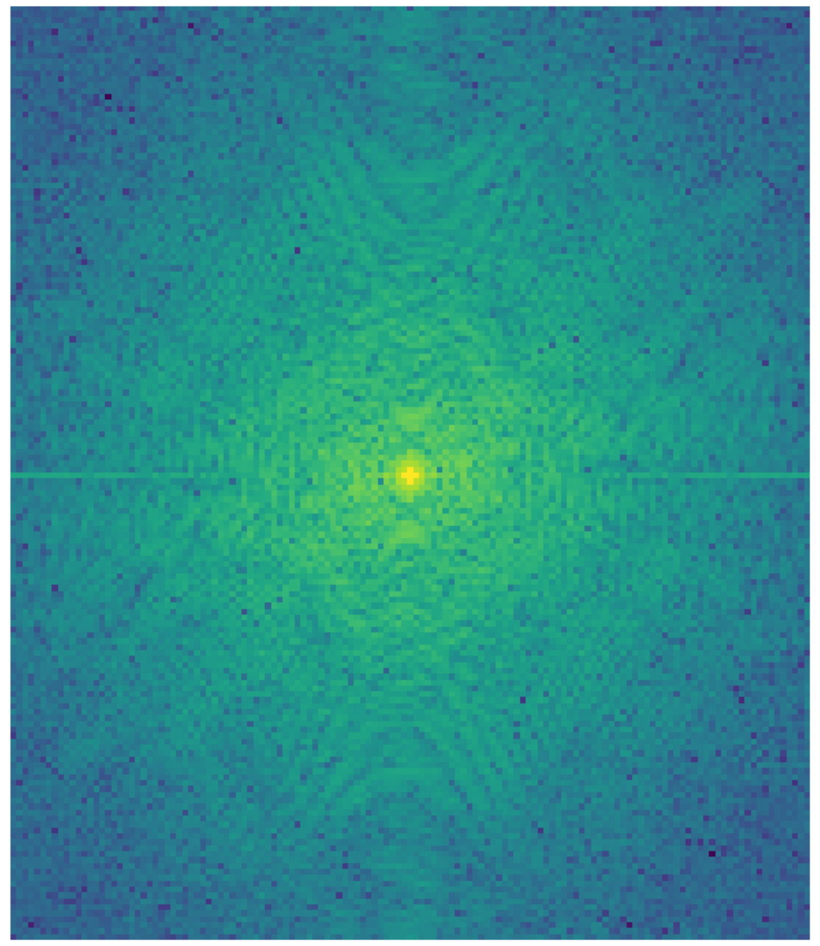

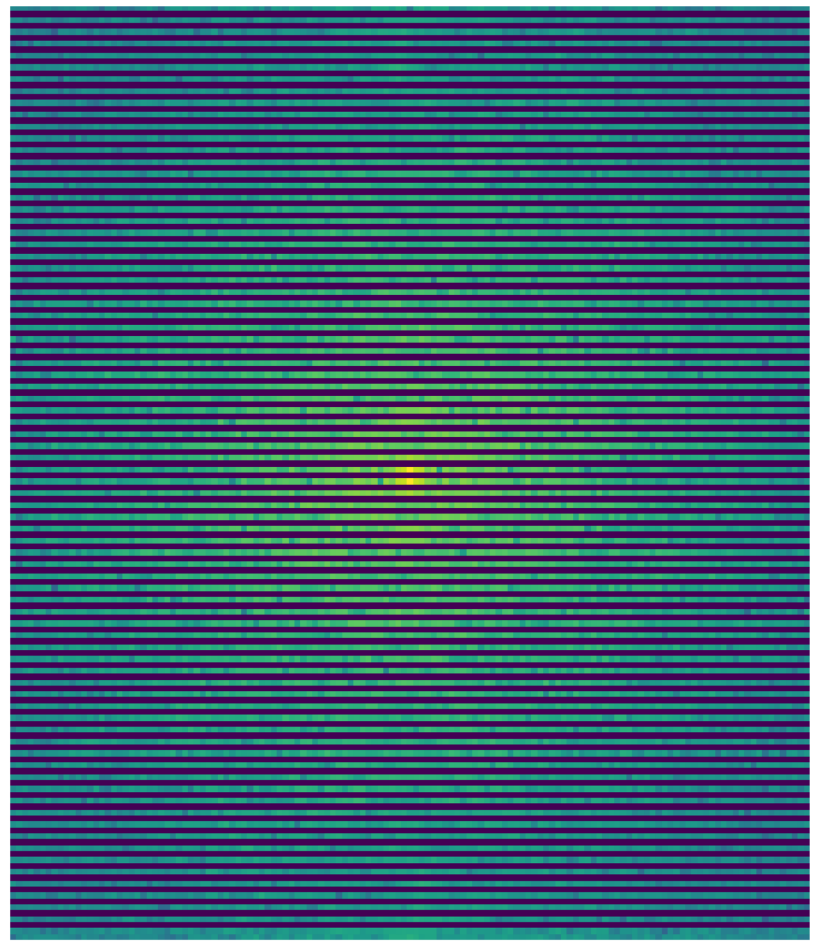

Sample every other row

Twice as fast, half the SNR

k-space FOV unchanged

Image-space voxel size unchanged

Twice the k_y spacing

Half the image-space FOV

Full image

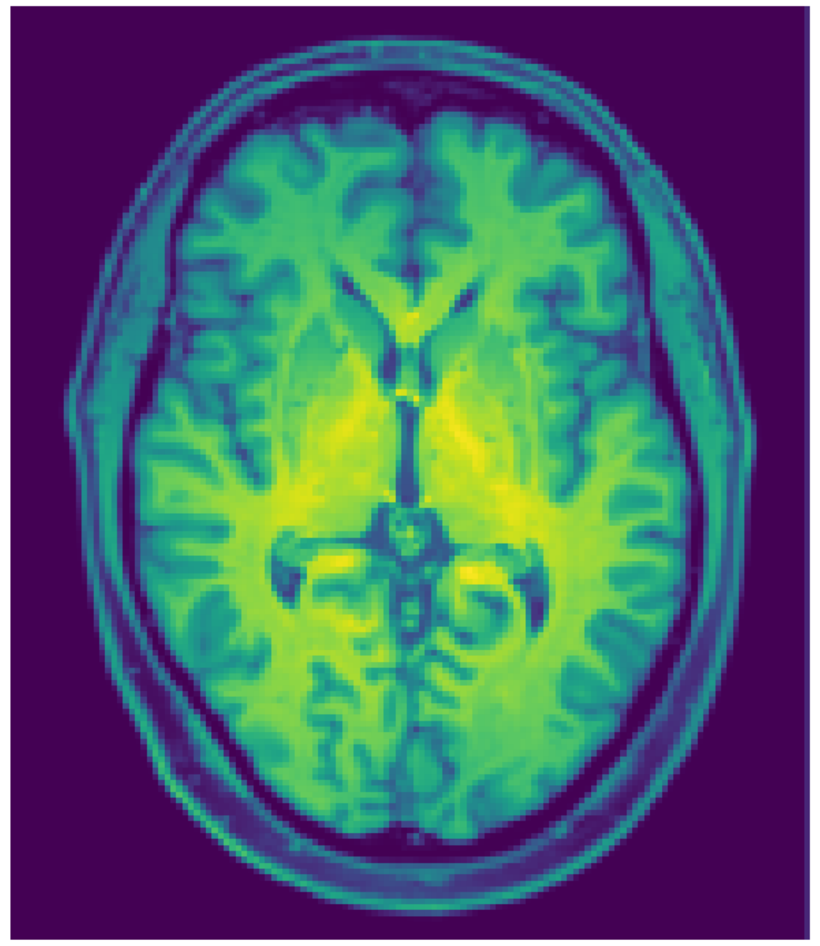

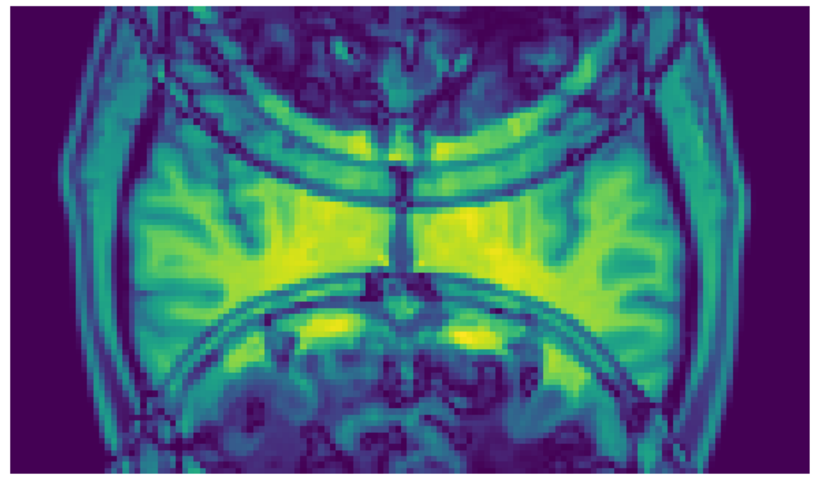

Half FOV with fold-over

SENSE Parallel Imaging

Reconstruction method that untangles fold-over using information multiple array coils

F = total signal in a coil image (known)

C = coil intensity weights (known)

A, B = weighted intensities from aliased voxels

I = actual intensities (unknown)

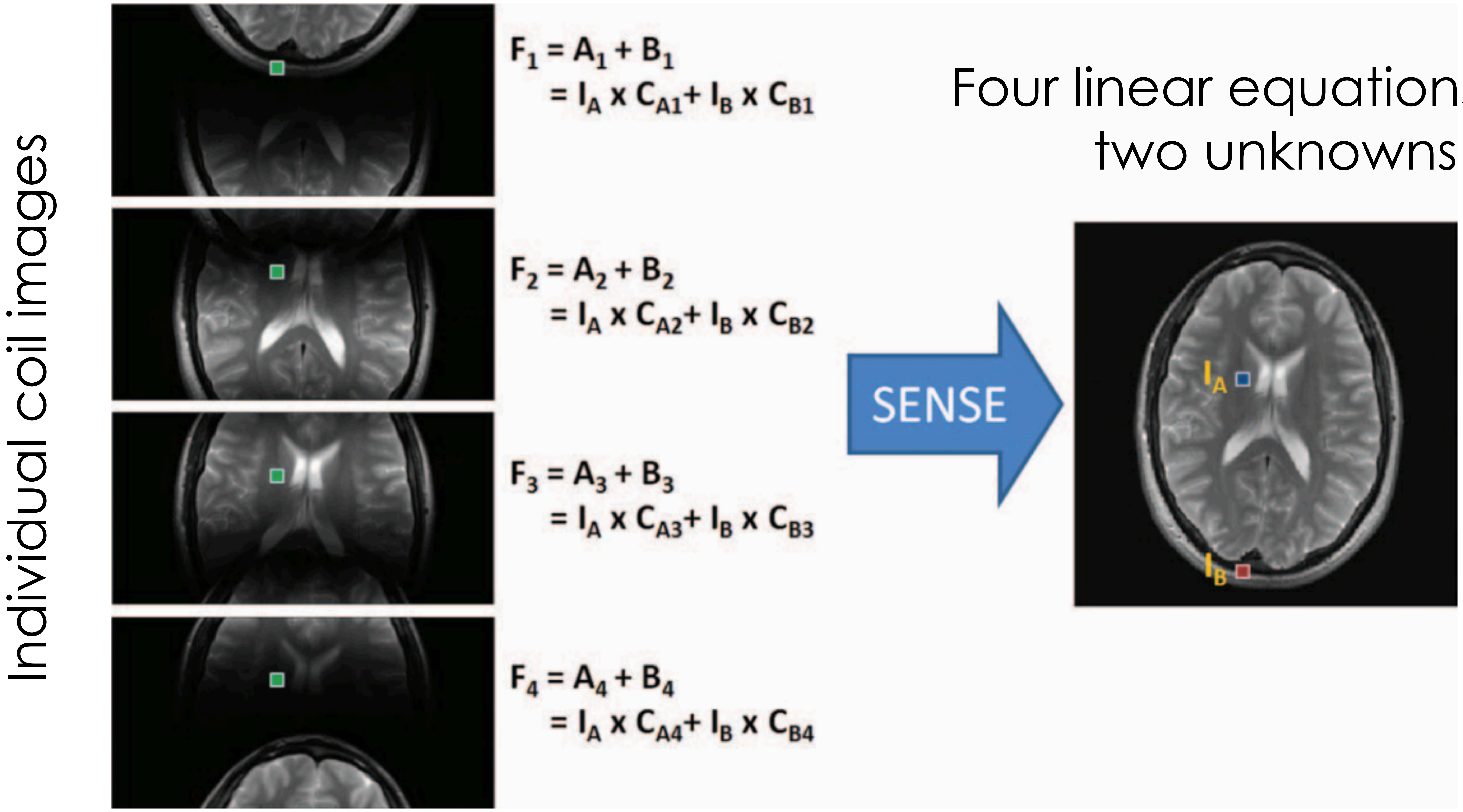

Deshmane, A., Gulani, V., Griswold, M. A., & Seiberlich, N. (2012). Parallel MR imaging. *Journal of Magnetic Resonance Imaging*, *36*(1), 55–72. https://doi.org/10.1002/jmri.23639

GRAPPA Parallel Imaging

Undersampled k-space for each coil

Auto Calibration Signal (ACS) for each coil acquired in advance

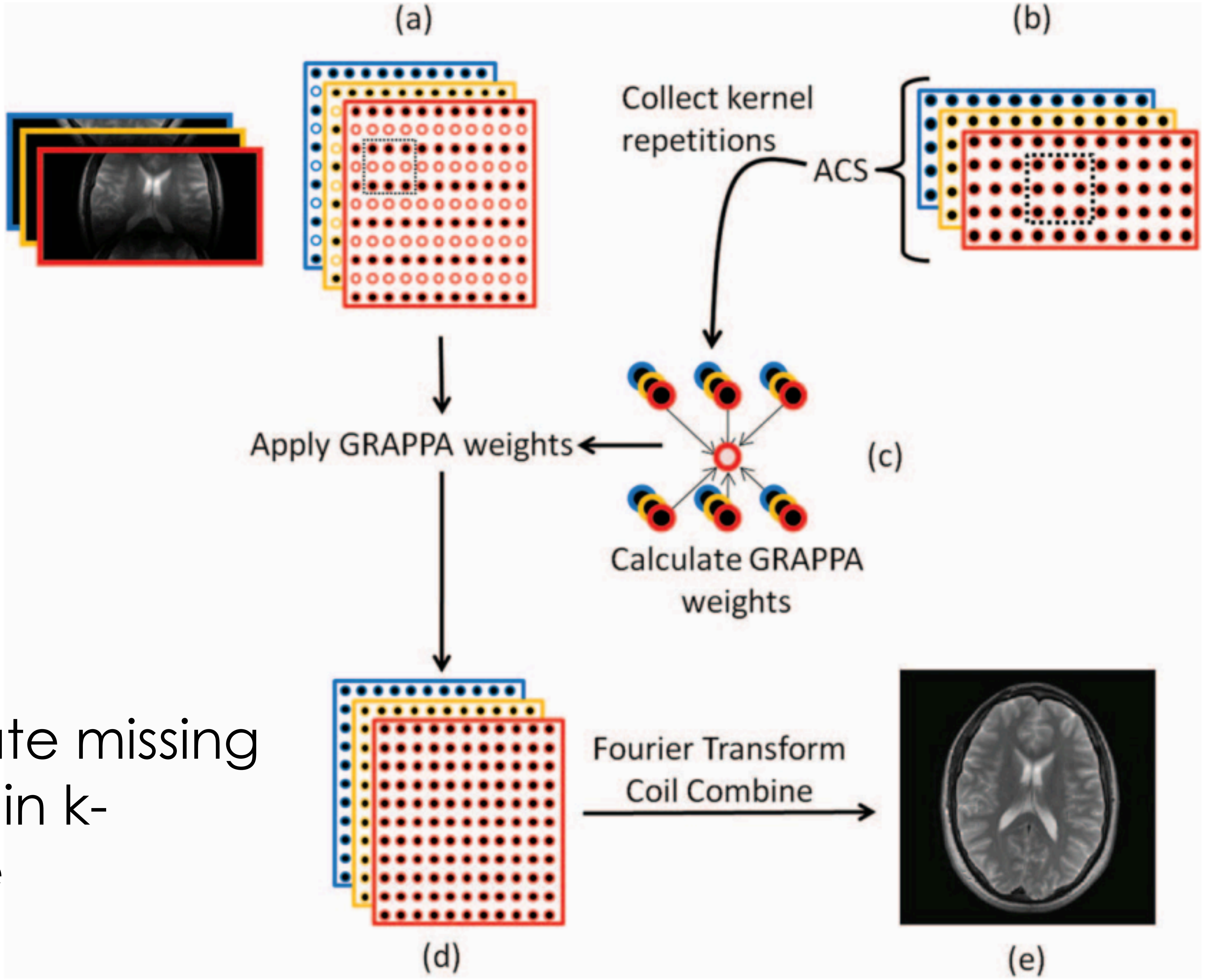

Estimate missing signal in k-space

Reconstructed full image

Pros and Cons of GRAPPA

- As the acceleration factor, R, increases:
  - EPI echo train shortens
  - Geometric distortion reduces
  - Minimum TR and TE reduce
  - SNR drops

$$\text{SNR} \propto \frac{1}{\sqrt{R}\ g}$$

g-factor and noise amplification

Measure of noise amplification due to parallel reconstruction

Spatial SNR

32 ch

8 ch

CP

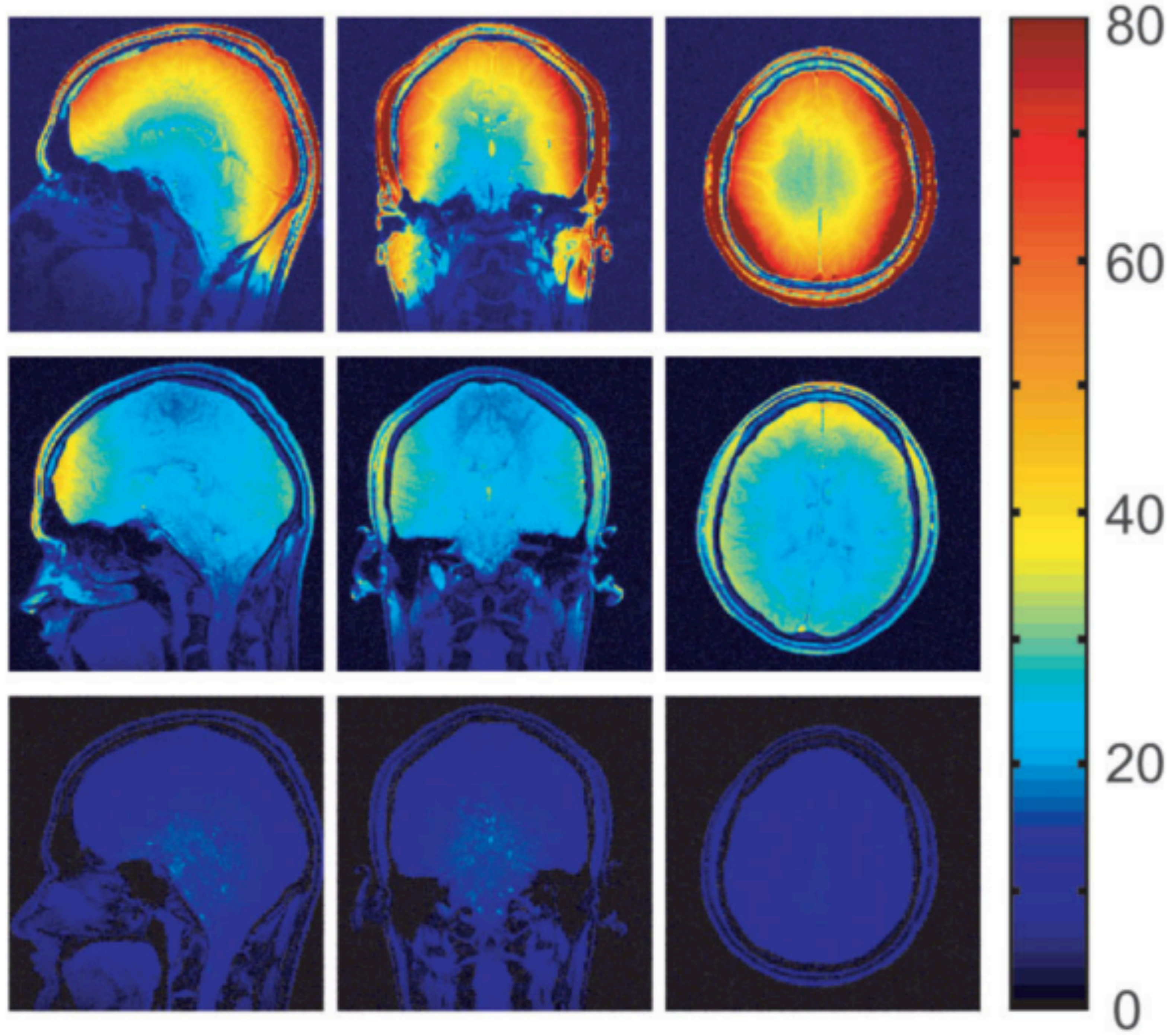

g-factor maps

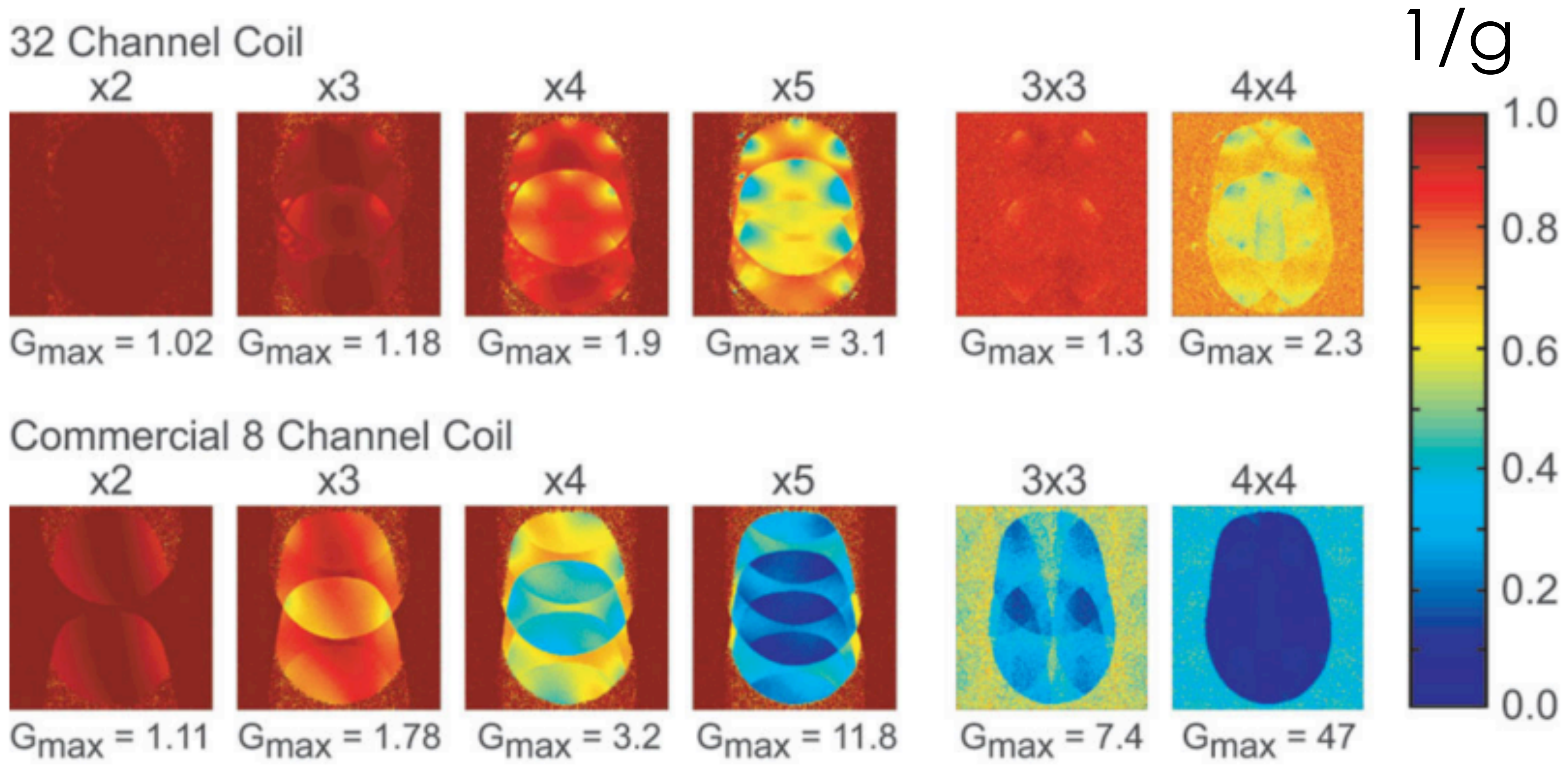

Wiggins, G. C., Triantafyllou, C., Potthast, A., Reykowski, A., Nittka, M., & Wald, L. L. (2006). 32-channel 3 Tesla receive-only phased-array head coil with soccer-ball element geometry. *Magnetic Resonance in Medicine: Official Journal of the Society of Magnetic Resonance in Medicine / Society of Magnetic Resonance in Medicine*, *56*(1), 216–223. https://doi.org/10.1002/mrm.20925

Multiband Slice Acceleration

RF pulses designed to excite multiple locations simultaneously

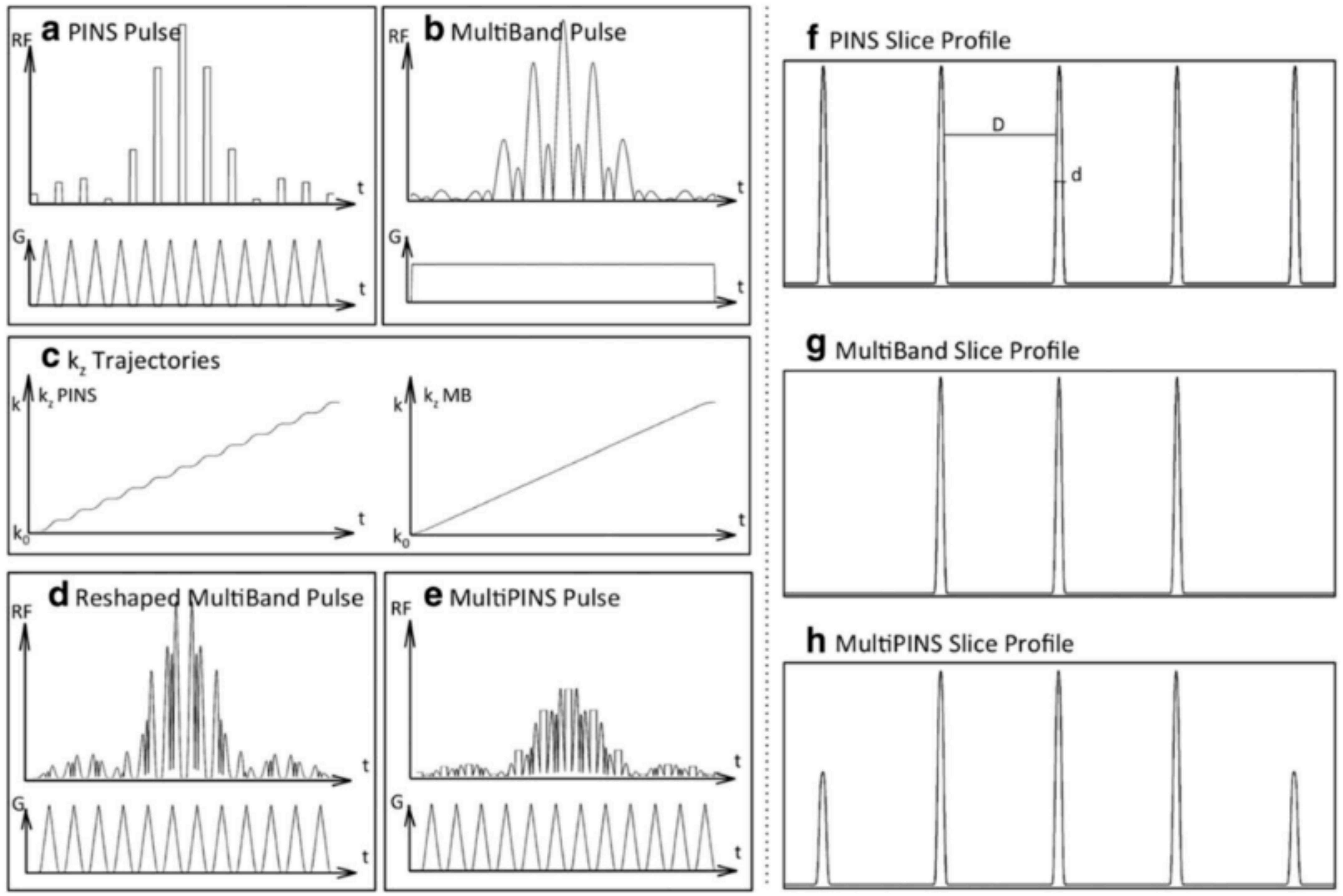

Excited slices combined in single image

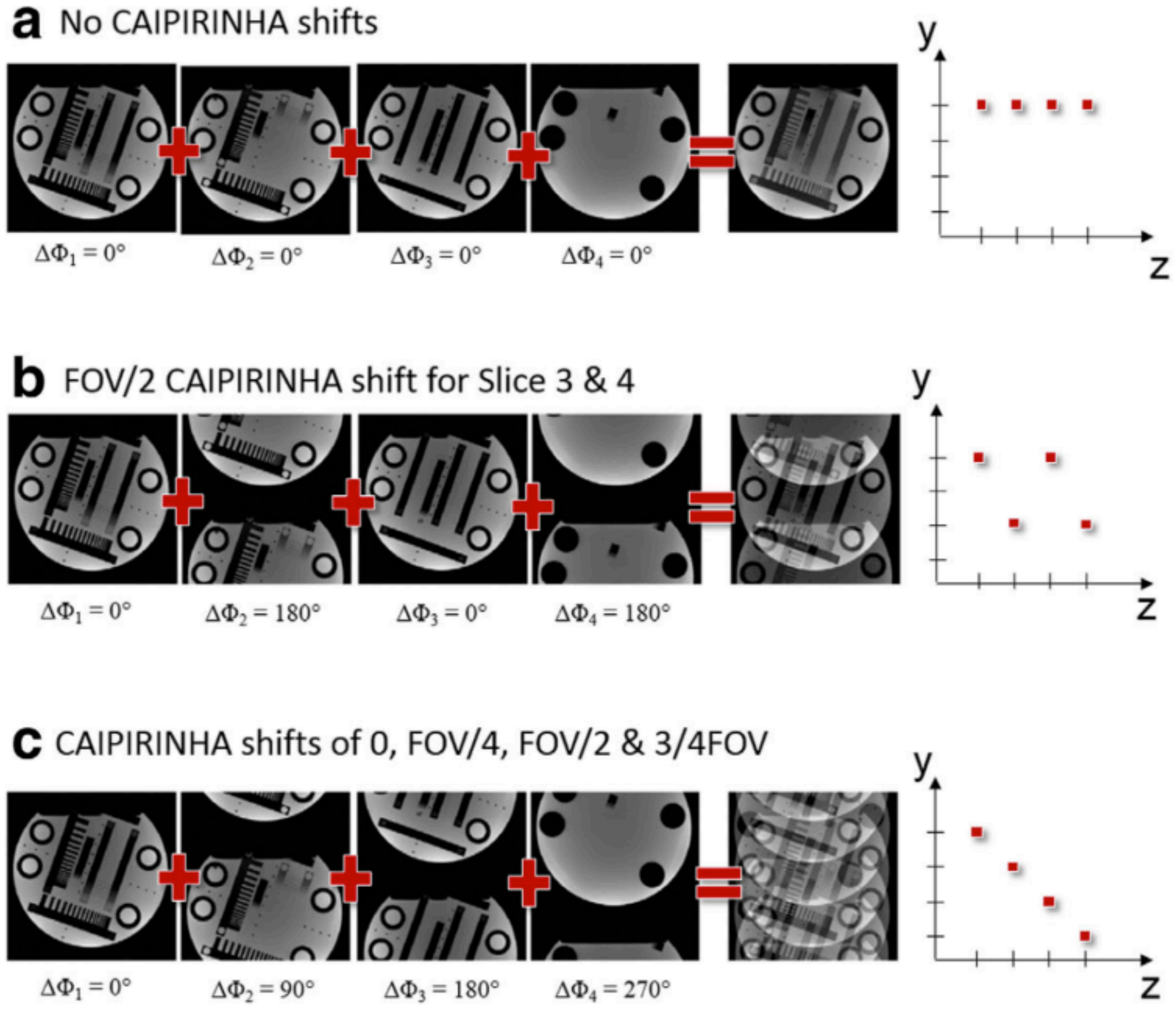

Multiband Slice Acceleration

Slice SENSE untangles overlapping slice images using information from individual array coils

[Can similarly use slice GRAPPA for k-space]

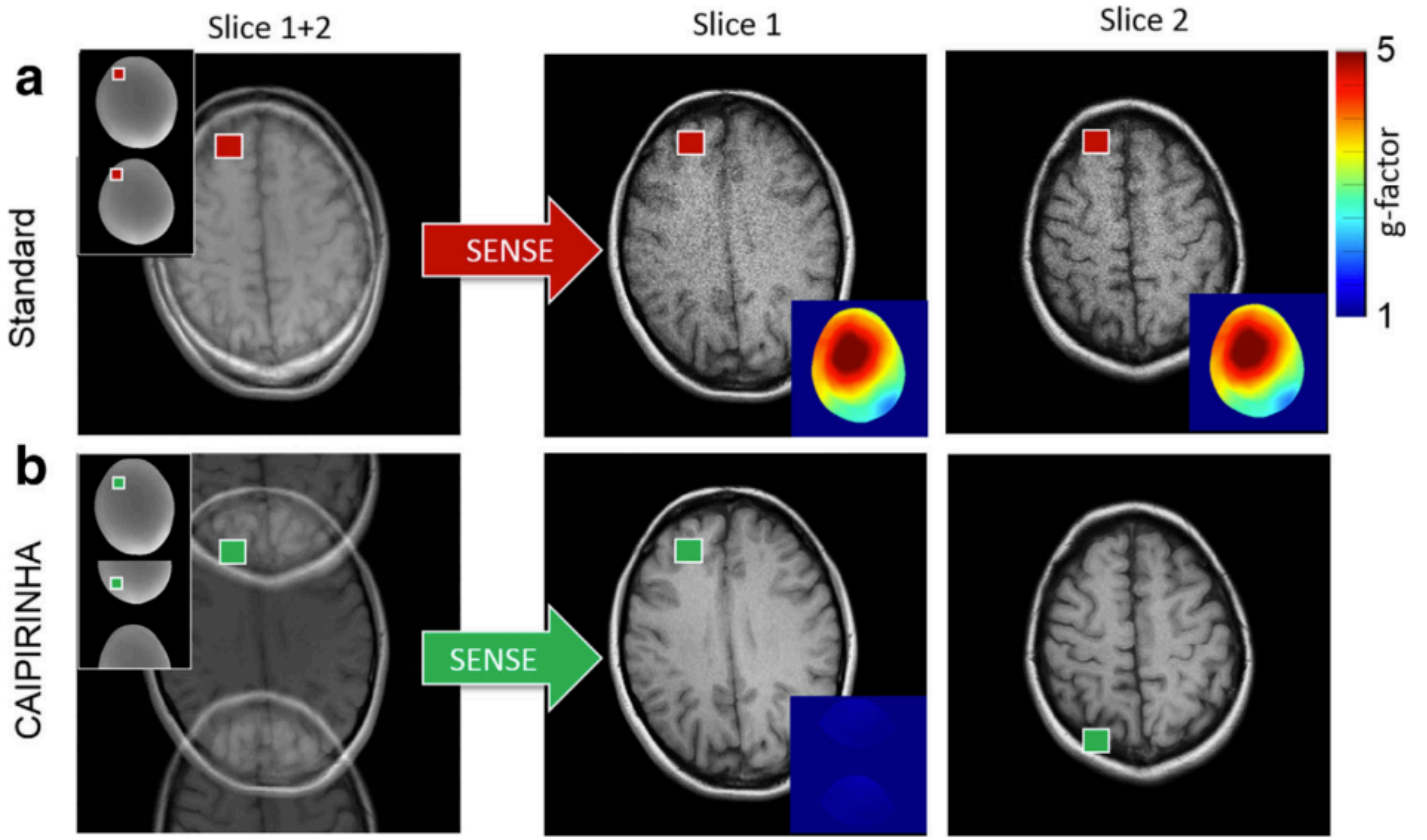

Very small g-factor and no 1/sqrt(R) penalty

Barth, M., Breuer, F., Koopmans, P. J., Norris, D. G., & Poser, B. A. (2016). Simultaneous multislice (SMS) imaging techniques. *Magnetic Resonance in Medicine: Official Journal of the Society of Magnetic Resonance in Medicine / Society of Magnetic Resonance in Medicine*, *75*(1), 63–81. https://doi.org/10.1002/mrm.25897

Next Time

- BOLD fMRI
- fMRI Preprocessing